

EXPERIMENTAL INVESTIGATION OF FRICTION FACTOR IN MICROTUBES
AND DEVELOPMENT OF CORRELATIONS FOR PREDICTION
OF CRITICAL REYNOLDS NUMBER

By

ATUL SINGH

Bachelor of Engineering in Mechanical Engineering

Rajiv Gandhi Technical University

Indore, Madhya Pradesh

2008

Submitted to the Faculty of the
Graduate College of the
Oklahoma State University
in partial fulfillment of
the requirements for
the Degree of
MASTER OF SCIENCE
December, 2011

EXPERIMENTAL INVESTIGATION OF FRICTION FACTOR IN MICROTUBES
AND DEVELOPMENT OF CORRELATIONS FOR PREDICTION
OF CRITICAL REYNOLDS NUMBER

Thesis Approved:

Dr. Afshin J. Ghajar

Thesis Adviser

Dr. David G. Lilley

Dr. Frank W. Chambers

Dr. Sheryl A. Tucker

Dean of the Graduate College

TABLE OF CONTENTS

| Chapter | Page |
|--|------|
| I. INTRODUCTION..... | 1 |
| II. LITERATURE REVIEW..... | 5 |
| III. EXPERIMENTAL SETUP & METHODOLOGY..... | 20 |
| 3.1 Details of Experimental Setup..... | 21 |
| 3.2 Calibration..... | 25 |
| 3.3 Experimental Procedure..... | 30 |
| 3.4 Experimental Uncertainties..... | 32 |
| 3.5 Constricted Flow Parameters..... | 37 |
| IV. RESULTS & DISCUSSION..... | 41 |
| 4.1 Diaphragm Effects..... | 42 |
| 4.2 Nickel Tube Results..... | 47 |
| 4.3 Comparison with Steel and Glass Data..... | 60 |
| 4.4 Roughness Effect in Laminar Region..... | 63 |
| 4.5 Correlations for Estimation of Critical Reynolds Number in Microtubes..... | 65 |
| V. CONCLUSIONS & RECOMMENDATIONS..... | 71 |
| REFERENCES..... | 74 |

LIST OF TABLES

| Table | Page |
|---|------|
| Table 1 - Transition range for different nickel tube diameters tested..... | 52 |
| Table 2 - List of earlier work done with low relative roughness tubes/channels..... | 56 |
| Table 3 - Lists error in friction factor values from the theoretical laminar line with and without correction factors..... | 64 |
| Table 4 - Lists critical Reynolds number measured experimentally and critical constricted Reynolds number calculated for glass and steel tubes..... | 67 |

LIST OF FIGURES

| Figure | Page |
|--|------|
| Figure 1 - Schematic of experimental setup..... | 21 |
| Figure 2 - Calibration curve for 125 psi diaphragm..... | 28 |
| Figure 3 - Calibration curve for 80 psi diaphragm..... | 29 |
| Figure 4 - Calibration curve for 50 psi diaphragm..... | 29 |
| Figure 5 - SEM image of 762 μm diameter Nickel tube..... | 36 |
| Figure 6 - Side view of micro tube with constricted parameters from Kandlikar et al. (2005)... | 37 |
| Figure 7 - Trend of proposed correlations for prediction of critical Reynolds number of Brackbill and Kandlikar (2007)..... | 39 |
| Figure 8 - Comparison of various diaphragms for 2083 μm steel tube of Ghajar et al. (2010a). | 43 |
| Figure 9 - Comparison of various diaphragms for 762 μm nickel tube..... | 45 |
| Figure 10 - Comparison of various diaphragms for 508 μm nickel tube..... | 46 |
| Figure 11 - Comparison of various diaphragms with focus on the transition region for 508 μm Nickel tube..... | 46 |
| Figure 12 - Experimental friction factor results for 1016 μm nickel tube..... | 48 |

| | |
|---|----|
| Figure 13 - Experimental friction factor results for 762 μm nickel tube..... | 49 |
| Figure 14 - Experimental friction factor results for 508 μm nickel tube..... | 49 |
| Figure 15 - Experimental friction factor results for 381 μm nickel tube..... | 50 |
| Figure 16 - Comparison of experimental data for 1016 μm , 762 μm , 508 μm and 381 μm nickel tubes..... | 53 |
| Figure 17 - Effect of diameter on friction factor profile of steel tubes from Ghajar et al. (2010a)..... | 54 |
| Figure 18 - Friction factor results for (a) Aluminum, (b) Silicon channels from Xu et al.(2000)..... | 57 |
| Figure 19 – (a) Glass and Silicon friction factors results from Li et al. (2003) (b) Glass and Silicon f.Re characteristics from Li et al. (2003)..... | 58 |
| Figure 20 (a) - Friction factor profile for fused silica and stainless steel tubes from Lorenzini et al. (2010)..... | 59 |
| Figure 20 (b) - Transition for fused silica and stainless steel tubes tested from Lorenzini et al. (2010)..... | 59 |
| Figure 21 - Comparison of experimental results for nickel tubes with steel tubes for (a) 1016 μm (b) 762 μm (c) 508 μm (d) 381 μm | 61 |
| Figure 22 - Comparison of 1016 μm diameter nickel tube with 1000 μm glass tube..... | 62 |
| Figure 23 (a) - Experimental original steel data plotted for comparison with the theoretical laminar region friction factor..... | 63 |
| Figure 23 (b) - Experimental steel data with constricted parameters plotted for comparison with the theoretical laminar region friction factor..... | 63 |
| Figure 24 - Comparison of critical Reynolds number for available data points with correlation proposed by Brackbill and Kandlikar (2007)..... | 65 |

Figure 25 - Linear fit for 0 to 0.5% relative roughness.....68

Figure 26 - Linear fit for 1 to 4% relative roughness.....69

NOMENCLATURE

| <u>Symbol</u> | <u>Description</u> | <u>Unit</u> |
|-----------------------------|---|--------------------|
| A | area | m ² |
| A _{cf} | constricted area | m ² |
| D | tube inner diameter | m |
| D _h | hydraulic diameter | m |
| D _{h,cf} | constricted hydraulic diameter | m |
| P _{cf} | constricted parameter | m |
| f | Darcy friction factor | |
| f _{cf} | constricted Darcy friction factor | |
| L | tube length | m |
| \dot{m} | mass flow rate | kg/s |
| V | average velocity | m/s |
| SEM | scanning electron microscope | |
| <u>Greek Symbols</u> | | |
| ϵ | roughness | m |
| ϵ_{FP} | roughness based on constricted parameters | m |
| ρ | density | kg/m ³ |
| μ | absolute viscosity | Pa.s |
| Δp | pressure drop across microtube | Pa |

CHAPTER I

INTRODUCTION

In recent decades micro devices have been a technological reality, size of equipment is condensing requiring the parts involved to be miniaturized. Equipment such as micro heat exchangers which is used for integrated cooling of electronic circuits, microfluidic systems like biochemical lab-on-a-chip systems, micro pumps and microelectromechanical (MEMS) systems. Advent of this micro era opened up new research area which was never explored before. Focusing on the research discussed in this thesis, condensing the size of mechanisms is steering use of conventional size of tubes towards micro tubes because of its extensive application. Applications like micro tubes/channels are used in reactant delivery, as biochemical reaction chambers, in physical particle separation, in inkjet print heads and for computer cooling chips. Functions involve pressurized flow through micro tubes/channels. Pressure driven flows through the micro tubes have flow characteristics of their own, which was not supported by any established macro tubes theories. Many studies were performed in last few decades for fundamental understanding of laminar, transition and turbulent region in micro tubes/channels, for better designing and development of micro devices. In the studies of flow characteristics in micro tubes/channels, roughness was found to be one of the major factors for variation in results from macro theories.

Looking at the literature many of the studies by Han and Lee (2006), Tang et al. (2007a), Ghajar et al. (2010a), Celeta et al. (2002), Brutin and Tardist (2003) performed in last few years suggest that friction factor for micro tubes deviate from the macro behavior for the tubes tested. Deviation behavior was prominent as the tube size was reduced meaning that deviation was maximum for smallest tube. Researchers Baviere et al. (2004) also found that many friction factor results were in agreement with the macro behavior. Whereas there were few studies by Choi et al. (1991) and Peng et al. (1994) who also established that micro tube friction factor was below the macro tubes behavior, contrary to the results expected from micro tubes. Observing this development is a hint that subject is far from having found an assured and agreeable answer. This further bolsters the fact that, there is a wide gap between the development of micro devices and the underlying physics.

In the present work one section of the study is investigating four nickel micro tubes with different inner diameter for roughness effects. Nickel tubes with relative roughness of 0.002 is relatively smoother micro tubes in comparison to steel tubes, and many other types of micro tubes/channels in the recent studies. The principal objective of this experimental portion of the study is to continue the ongoing and demanding, research on flow behavior through microtubes worldwide for a better picture of flow behavior through microtubes. Ultimately leading to improvement in micro-manufacturing techniques. It involves exploring transition region flow along with laminar region flow behavior of nickel microtubes. It's accomplished by measuring pressure drop over a wide range of Reynolds number from laminar to turbulent region. The discussed experimental work on nickel tubes in this thesis is an addition to the study carried out by Ghajar et al. (2010a), who worked on much rougher steel tubes. Present work takes it to the

next level by measuring friction factor for smooth tubes, and comparing it with previous steel work to realize difference in flow regimes due to roughness.

One flow regime in micro flow regimes, which has been mostly declared as no roughness effect was laminar region. Amidst all the skepticisms surrounding the flow characteristics in microtubes, it's rather questionable to conclude no roughness effects in laminar region. Kandlikar (2005) scrutinized the studies by Nikuradse (1933) and researchers from 1980's and 1990's. It was acknowledged by author that inattention to experimental uncertainties and flow parameters by the researchers, steered to the conclusion that flow in laminar region follows along the theoretical lines. Ghajar et al. (2010a) study mainly concentrated on transition region but it was observed by the authors that roughness had effects in laminar region, similar was observation of Yu et al. (1995). This perplexity of flow in laminar region has emerged a new attribute in study of flow characteristics through micro tubes/channels, apart from studying transitional region of the flow in micro tubes/channels.

Second section of this work is an attempt to understand better laminar region characteristics. In the above mentioned and most of the studies performed on micro tubes/channels, the inner diameter used for calculations of friction factor was the inner diameter itself. Also surface irregularities which have been acknowledged of having strong effects in transition region of micro tubes/channels, has been neglected completely for laminar region. Kandlikar et al. (2005) introduced three parameters called as constricted flow parameters representing roughness effects for ϵ/D greater than zero. These three parameters in a nutshell overlook the roughness element height and a free flow area is considered. A new equation was also proposed for calculation of friction factor in this free flow area. Reduction of uncertainty in calculation of friction factor in

laminar region is expected from use of this equation. The equation was employed on the data for nickel tubes (low relative roughness), previous data of Ghajar et al. (2010a) for steel tubes (high relative roughness) and on glass tubes (low relative roughness) data obtained from University of Macau, China. This analysis prime objective is to investigate the equation meticulously for a better insight in this area of low Reynolds number. Furthermore the source behind the change in results by using the equation can be understood.

This write up is divided into four major chapters. The chapter two is a comprehensive literature review of work done on micro tubes/channels flow characteristics. Chapter three elucidates experimental set up involved in obtaining pressure drop readings and uncertainties associated with it. Also evolvement of new friction factor equation from constricted flow parameters is discussed in Chapter Three. In Chapter Four results assimilated from pressure drop readings for nickel tubes is analyzed and discussed. It includes studying effects of different inner diameter in transition regime, and outcome of using the constricted friction factor equation and cause behind the changes in results of laminar regime. Chapter five is the conclusions drawn from the present work and recommendations for future possible work in this area of research.

CHAPTER II

LITERATURE REVIEW

Fluid flow and studies related to it has always been a very important research subject starting as early as in 1700 with Bernoulli giving one of the fundamental equations. However with industrialization and introduction of automobile study of fluid flow in pipes was very important because of its extensive application. It was studied comprehensively by Poiseuille, Darcy, Fanning, Colebrook and Moody to name a few. In 19th century Darcy performed pressure drop experiments on pipes of different materials and roughness and he was first to give the concept of relative roughness. Fanning proposed a correlation for the pressure drop as a function of surface roughness. One of the phenomenal works was done by Moody by representing in a graphical format that relates the Darcy's friction factor, Reynolds number and relative roughness for fully developed flow in a circular pipe, providing engineers with a convenient method of determining pressure drop with respect to friction factor. Researches were sufficient up till the introduction and boom in technologies requiring small diameter tubes in the range of 500 μ m and below.

At such small diameters results of manufacturing processes like roughness projection on the machined surfaces play a very considerable role in transport phenomena. Parameters like surface roughness, Reynolds number and flow regime with the size of tube diameter develop into very

important factors. The chart developed by Moody known as Moody's chart, Darcy equation and all the old work were not sufficient anymore for micro tubes.

Lack of sufficient study and behavioral knowledge of flow in micro tubes led to many researchers dealing with fluid flow to plunge into this unknown territory. Looking at the literature early researches observed lower friction factor than theoretical predictions while later researches found friction factor higher than theoretical predications and some of them found friction factor agreeing with theoretical results. This wide spread disparity was reviewed in detail by Krishnamoorthy and Ghajar (2007). In recent years Kandlikar et al. (2005) suggested a new way of looking at flow cross section so that better friction factor can be calculated, this all is directing towards the scope of work left in this area.

Starting with one of the earliest works Wu and Little (1983) working on Silicon and Glass micro-channels of trapezoidal cross section with hydraulic diameters ranging from 55 μm to 73 μm of different roughness and passing gas as the fluid. Results have indicated higher friction factors in the laminar region by 30% of theoretical values and in turbulent region 10% of theoretical values, for the silicon channels and 3-5 times higher for glass channels with early transition for both types of channels. The authors conclude that the roughness whether evenly distributed or discrete is an important factor in the flow through micro-channels. Rougher channels have exhibited earlier transition, but the measurement of roughness is not believed to be very accurate.

Acosta et al. (1985) investigated nitrogen flow through a rectangular stainless steel channel with hydraulic diameter of 953 μm and relative roughness ranging from 0.13% to 5.2%. For smaller relative roughness i.e. 0.13% and 0.21% laminar regime followed along with the theoretical

lines. Whereas friction factor for 2.4% and 5.2% relative roughness was considerably higher from the theoretical lines. Reynolds number ranged from 1300 to 22000.

In 1990's many researchers found the friction factor data below the theoretical values. Choi et al. (1991) performed pressure drop measurements on fused-silica micro-tubes with diameters ranging from 3 to 81 μm and dry-nitrogen gas as the test fluid. A controlled roughness measurement using the images produced by the laser interferometric microscope indicated very low roughness values, thus concluding the tubes to be smooth. The friction factor results for all the tubes measured were found to be less than the theoretical predictions, with the smallest tube showing the largest variation. The $f \cdot \text{Re}$ value obtained was in the range 50-53 for all the tubes tested, which is considerably less than the theoretical value of 64. Also it should be noted that the authors found that readings are not influenced by the roughness of the micro-tubes.

Peng et al. (1994) investigated the water flowing through rectangular micro channels with hydraulic diameters of 0.133-0.367 mm and height to width (H/W) ratios of 0.333-1. Results observed were that transition was found to occur early as compared to regular channels; also transition region is shortened to smaller Reynolds number zone. Laminar and turbulent friction factor deviated from the classical theories. It was noted by the authors that there was a special range of ratio H/W 0.5 mm approximately at which the experimental data was lower than the theoretical correlations.

Arkilic et al. (1994) passed helium through silicon micro channels and suggested that no slip boundary condition of the Navier-Stokes equations fails to estimate the mass flow for the given inlet and outlet pressures. It was suggested by them that slip flow should be introduced at the

wall which was derived from momentum balance and this resulted in decrease in friction factor for micro channels even less than the conventional predictions.

Yu et al. (1995) investigated fluid flow and heat transfer characteristics through 15, 52 and 102 μm micro tubes, with Reynolds number ranging from 250 to 20000. Looking at fluid flow results for laminar region it was observed that the results are below the conventional value of 64 for $f \cdot \text{Re}$. It was suggested by the authors that for micro tubes the roughness has a serious effect on friction factor in laminar region as observed by Wu and Little (1983) so flow cross section needs to be recalculated. Transition starts at 2000 Reynolds number, also in turbulent region there was similar case like laminar region the friction factor was lower than theoretical.

Harley et al. (1995) investigated experimentally and theoretically low Reynolds number, high subsonic Mach number, compressible gas flows in silicon micro channels with nitrogen, helium and argon gases. Micro channels were 100 μm wide, 10^4 μm long and the Knudsen number ranged from 10^{-3} to 0.4. Numerical solution indicated that pressure may be assumed to be uniform in the channels cross-sections perpendicular to the flow direction, it should be noted that it was a 1-D flow analysis. Experimentally the data was 8% less than the theoretical predictions of the friction constant.

Mala and Li (1999) investigated flow through fused silica and stainless steel micro tubes with diameters from 50 to 254 μm . It was seen that there is a disparity between experimental results and Poiseuille flow equation in the laminar range. Two reasons were suggested by the authors either the flow is going in an early transition or there is surface roughness effect on micro tube flow. Both the phenomenon was backed up by different theories and researches by other investigators, a roughness viscosity model was proposed to explain roughness effect.

Papautsky et al. (1999) analyzed the behavior of fluid flow in a rectangular micro channel with a numerical model developed based on micropolar fluid theory and then compared it with experimental results. Numerical model predicted flow characteristics, such as volumetric flow rate, average velocity, pressure drop and Darcy friction factor. It was observed that numerical model predicted experimental results 47% better than Navier-Stokes theory, when compared with the theoretical results.

Du et al. (2000) studied nitrogen in glass microtubes with diameter of 80.0 μm - 166.3 μm . The measured relative roughness was $< 0.1\%$. The friction factor and transition Reynolds number were in good agreement with classical theory predictions. Transition was reported at 2300 Reynolds number, it was also reported that no early transition was observed.

Xu et al. (2000) conducted experiments on Aluminum channels with hydraulic diameter 50-300 μm and Silicon micro channels with hydraulic diameter 30-60 μm . Surface roughness for aluminum channels was 0.5 μm and for silicon channels it was 20 nm. For laminar region the results were in good agreement with Poiseuille law deviation from laminar was observed at around 1500 Reynolds number. For smaller channels there was no early transition as it was anticipated based on previous studies, but the friction factor for aluminum channels was higher than silicon channels. It was noted by the authors that shape and size of tube or channel can disturb the behavior of the flow from conventional theory. Also for Navier-Stokes equation it was observed that it is not suitable to predict the flow characteristics for diameter bigger than 30 μm for micro channels.

Pfund et al. (2000) performed experiments across rectangular micro channels with hydraulic diameters of 128–521 μm using water as the fluid. Relative roughness was in the range of 0.57%

to 5.71%. Reynolds numbers were between 60 and 3450. For the largest channel with $D_h = 521$ μm and least relative roughness of 0.57%, the friction factors reported were in reasonable agreement with the theoretical value, with an increase in friction factor of less than 8%. However for rougher channels with higher relative roughness between 1.14% and 5.71%, the increase in friction factor from theoretical ranged from 10% to 25%. Transition was reported to occur at lower Reynolds number than for macro channels.

Araki et al. (2002) while working on polymer electrolyte membrane (PEM) fuel cells emphasized on the importance of micro channels, and suggested that flow regime of micro channels and micro tubes is an area which requires continued research.

Hegab et al. (2002) studied refrigerant R134a flow in aluminum rectangular channels with hydraulic diameters ranging from 112–210 μm , and relative roughness ranging from 0.16% to 0.89%. Reynolds number ranged from 1280 to 13,000. Data points collected in the laminar regime for friction factor were in good agreement with the predictions of classical laminar flow theory. But in the transition and turbulent regimes, the friction factor was 9–23% lower than convectional correlations. Transition was reported around 2000-4000 Reynolds number.

Celata et al. (2002) investigated hydraulic and thermal characteristics of 130 μm inner diameter capillary tube with refrigerant R114. Only hydraulic portion is discussed here. Fluid was entered the inlet section at two different temperatures 17°C and 33°C. It was observed by the authors that the laminar region friction factor values were in extremely good agreement with Hagen – Poiseuille theory for Reynolds numbers less than 580, but for Reynolds numbers less than 100 – 200 moderate deviation was noted. It was explained by the increase in the data acquisition error at low flow rates. It was also brought into light by the authors that in micro tube even smooth

surface can be characterized as rough because of high value of relative roughness. Transition was found to occur at 1880-2480 Reynolds number with respect to two different temperatures. Turbulent regime was found slightly over predicted when compared with Blasius correlation. It was concluded by the authors that further systematic studies are required for better knowledge of flow structure in micro tubes.

Li et al. (2003) ran experiments on glass, silicon and stainless steel with inner diameter ranging from 79.9-166.3 μm for glass, 100.25-205.3 μm for silicon and 128.76-179.8 μm for stainless steel. Results observed were that there was no difference in the smooth micro tubes behavior from that in macro tubes for diameter larger than 80 μm . For rough micro tubes it was 15-37% larger than theoretical values. Transition was observed at 1700-2000 Reynolds numbers, which concludes that there was no early transition.

Brutin and Tardist (2003) performed experiments on fused silica micro tubes with diameters ranging from 50-530 μm . Two fluids (tap and distilled water) were used and it was distinguished by the authors that there was disparity from classical behavior because of ionic composition of fluid. It was observed that ionized fluid (tap water) had effect on flow and caused it to deviate from the conventional theories whereas this was not the case for deionized fluid (distilled water). Also surface polarity was found as the reason for disparity with the theories. It should be noted that surface roughness was not mentioned as one of the prime reasons for deviation from conventional theories.

Wu and Cheng (2003) measured friction factors for silicon micro channels for hydraulic diameters in the range of 25.9–291 μm , with trapezoidal cross-section. They concentrated in the laminar region, fluid used was deionized water. The relative roughness of tested micro channels

was $\leq 0.12\%$. Authors concluded that experimental data being within $\pm 11\%$ of theoretical predictions was in good agreement. Transition from laminar to turbulent flow was found to occur at Reynolds number range of 1500–2000, for hydraulic diameters of 103.4 μm - 291 μm .

Phares and Smedley (2004) tested deionized water, tap water, saline, and glycerol/water mixture flow through circular micro tubes of stainless steel and polyimide. Diameter of tubes ranged from 120–440 μm whereas relative roughness ranged from 2.5% to 1.8% for stainless steel whereas for two polyimide tubes with $D = 119$ and $152 \mu\text{m}$, the relative roughness was less than 1%. Authors focused in the laminar region. It was concluded that measured friction factor in polyimide tubes was in good agreement with the theoretical predictions, although the friction factor in stainless steel tubes had 17% deviation from the conventional theory.

Baviere et al. (2004) investigated flow through stainless steel micro tubes of 125, 300 and 500 μm . Only laminar regime was investigated with 800 Reynolds number. Looking at the results it was found that for 125 and 300 μm they were in good agreement with conventional laminar theory. $f \cdot \text{Re}$ value was near 60, also there was no early transition.

Zhigang and Yaohua (2005) performed experiments on quartz glass micro tubes with inner tube diameters of 315 and 520 μm . In the experiments apart from pressure drop measurements they also visualized the flow field by a CCD camera to observe the laminar to turbulent transition. Flow transition was observed by the flow visualization and it was found that for 315 μm transition Reynolds number was 1278 and turbulent Reynolds number was 1562 and for 520 μm transitions Reynolds number was 1493 and turbulent Reynolds number was 1724. Looking at the friction factor results it was 10-25 % higher than that predicted by the classical laminar theory, and it was 10-25 % lower than that predicted by Blasius for turbulent region.

As mentioned by Wu and Little (1983) in their conclusion that roughness can be distributed in anyway. It raised many questions at the friction factor obtained by previous authors so Kandlikar et al. (2005) discussed a different way of looking at the diameter. It was proposed by them that entire cross section of inner diameter which is taken directly into the calculations of friction factor in micro tubes cannot be correct. Roughness layers on the wall of the micro tubes, which causes a flow area constriction so the entire cross section cannot be considered for friction factor calculation. There were three parameters proposed to characterize the surface roughness, and three parameters to characterize the hydraulic diameter as well. Parameters were based upon height of projections from the rough surface. When this constricted diameter was used in a rectangular channel diameter from 325 μm to 1819 μm with air and water as working fluids, it was observed that the flow which was not in agreement with the theoretical data is now within an error range of 5% for laminar region. In turbulent region there was very little effect of constricted flow diameter as the flow was still greater than 30% deviated from the theoretical data. It was concluded that flow does seem to interact with base walls. For transition region it was observed that flow goes in an early transition due to constricted diameter. It was noted by the authors that further experimental data and analysis is needed. For recommending any specific set of characteristics which represent the flow effects due to surface features in micro tubes/channels.

Brackbill and Kandlikar (2006) continued further study with hydraulic diameter in the range of 424 μm to 2016 μm emphasizing on transition to turbulent flow at low Reynolds numbers and the friction factor caused by triangular roughness elements of different pitch (405 μm and 815 μm). It was seen in the results that with just using the hydraulic diameter there was an error with the theoretical values but when constricted hydraulic diameter was used as proposed by Kandlikar et

al. (2005) a better fit was obtained for both the pitches. Transition to turbulence showed a distinct difference in transition Reynolds number and in the section after the departure from the laminar flow.

Han and Lee (2006) investigated flow of distilled water through Polyetheretherketone micro tubes with 87 and 118 μm diameter tubes, surface of the tubes was considered as hydraulically smooth as the roughness height was not more than 5 μm . Experiments were carried out focusing on the laminar region with Reynolds number 15-450 for 87 μm and 60-1300 for 118 μm diameter tubes. Frictional pressure loss was within the 10% range of macro tubes. There was no early transition detected within the tested range of Reynolds number.

Brackbill and Kandlikar (2007) did more experiments on mini channels with 30 to 1700 μm hydraulic diameters further bolstering the theory of constricted flow parameters by Kandlikar et al. (2005). Reynolds number varied from 30 to 1700 and it was seen that there is effect of roughness in the laminar region friction factor contrary to Nikuradse's (1933) results. Friction factor was observed to be predicted accurately by constricted flow parameters.

Tang et al. (2007a) performed experiments with nitrogen and helium flows on Silica micro tube ($D = 50\text{-}201 \mu\text{m}$), square micro channels ($D_h = 52\text{-}100 \mu\text{m}$) and stainless steel micro tubes ($D = 119\text{-}300 \mu\text{m}$) to check the roughness effect concentrating in laminar region. Results concluded by them were standard. For fused silica tube in laminar flow regime all results were in good agreement with the predictions. Transition was slightly earlier than conventional size tubes, it's also mentioned that within the tube/channel sizes used in the experiment there is no clear size related increase or decrease trend regarding the deviation between the experimental results and

theoretical predictions. For stainless steel tubes the friction factor is significantly (28-70%) higher than theoretical predictions and this was attributed to surface roughness effect.

Tang et al. (2007b) teamed up again and experimented with fused silica with diameters of 50-100 μm and stainless steel tubes with diameters of 373-1570 μm . Relative roughness for stainless steel tubes was 0.95%, 1.4%, 2.4% whereas fused silica was considered to be smooth. For fused silica tube it was observed that experimental friction factor was in good agreement with a deviation of $\pm 10\%$ from the theoretical results. For stainless steel tubes it was seen that relative roughness can be neglected if relative roughness is less than 1.5% in micro tubes. And for relative roughness greater than 1.5% roughness effect there was a deviation of more than $\pm 10\%$ from the theoretical results. It was concluded that measured friction factor deviation from theoretical results is caused by geometrical ingredients.

Lorenzini et al. (2010) analyzed water flowing through stainless steel and fused silica tubes inner diameter ranging from 29-508 μm . Fused silica was the smooth tube and stainless steel tube was rougher. Pressure drop experiments were performed over the range of Reynolds number (30-1000) with five different pressure transducers to get accurate pressure drop readings. It was observed that in laminar region the experimental data was in agreement with Poiseuille equation except for micro channels less than 100 μm it tends to deviate a little. It was concluded by the authors that friction factor in the laminar region is independent of surface finish. In laminar to turbulent transition two types of transition were observed one was smooth transition and second abrupt transition. Gradual transition was observed for smooth transition whereas sudden departure of flow from laminar was observed for abrupt transition. Abrupt transition was more dominating for critical Reynolds number higher than 2300. Smooth transition was the case for fused silica tubes and rough transition for stainless steel tubes. There was no case of earlier

transition than the one predicted by the classical theory. Critical Reynolds number was found to be in the range of 2160-4370. One of the key points to note is that in stainless steel tubes a contradictory behavior was observed, there was a delay in transition even though the tubes are rougher than fused silica, and previous researches have shown that early transition occurs for rough tubes. In turbulent region for smooth tubes it was in very good agreement with Blasius equation, but for rough tubes it was noted that experimental values of the friction factor were independent of the Reynolds number in turbulent region. Reason behind this was stated as the surface roughness of sudden asperities of irregular shape, with short wavelength and relatively high amplitude.

Rebecca and Kandlikar (2012) investigated the flow through artificial structured roughness in micro channels, to understand the effect of height, slope and spacing of roughness on fluid flow. Hydraulic diameter for the experiments ranged from 452 μm to 1745 μm , pitch (150 – 400 μm) and height (36 – 131 μm), Reynolds number ranged from 5 – 3400. A theoretical model (wall function method) was proposed by authors to predict the effect of surface features on the friction factor. This model was validated by the experimental results conducted on micro channels, with different pitch to height ratio (λ/h) for different roughness. Authors recorded many frictional losses by varying the pitch to height ratio and changing the aspect ratio. Frictional losses were compared with wall function method. Method worked reasonably well predicting friction factor for good number of variations. But for one pitch to height ratio discrepancies from theoretical was large which was unexpected, this pitch to height ratio was in the middle of the range tested. This was explained by fluid recirculation between the roughness elements with the main flow in the core which introduced additional losses. Whereas for lower and higher pitch to height ratio values the recirculation effects seemed to be contained between the roughness element itself.

With all the data collected in the experiments still there is no clear picture of when do we see transition depending upon the diameter of the tubes. Looking at the investigation and results obtained by different researchers it can be observed that most of the researchers agree that macro tubes theories do not apply to micro tubes and channels, and it has been noticed by all the authors that roughness plays a major role in fluid flow in micro channels and tubes. There were researches by Yu et al. (1995) and Pfahler et al. (1991) showing that in few cases flow through micro tubes/channels showed behavior below the conventional theories.

But there has been no concrete research giving a distinguished mark according to diameter and roughness for micro tubes/channels asserting a range in which micro flow behavior can be seen, and diameter from where it is not micro in nature. Also the start and end of transition was one question unanswered by many authors. To answer these questions Ghajar et al. (2010a) investigated flow through a complete range of stainless steel tubes having 12 different tubes with diameters ranging from 2083 μm to 336 μm and water as the working fluid. Importance of accuracy while collecting pressure drop data, measurement sensitiveness was brought to light by the authors. It was noted that with pressure sensing diaphragm it is necessary to collect pressure drop data for entire pressure sensing range before changing to next one, it enhances the collection of accurate data. Experimental results indicated that start and end of transition region was influenced by the tube diameter. Friction factor was in agreement with the conventional theories from 2083 μm to 1372 μm however after 1372 μm to 336 μm tube diameters, roughness kicks in and friction factor moves away from the conventional theories. Reynolds number range gets narrower as the tube diameter decreases.

Based on the work of Ghajar et al. (2010a) a complementing study was performed by Ghajar et al. (2010b). Experiments were performed on glass microtubes of 1000 μm diameter with five

different roughness values ranging from 0 to 4.3 μm . It was concluded by the authors that surface roughness has effect on start and end of transition, also it was noted that transition region grows narrower for increased roughness. In this thesis the work mentioned for stainless steel tubes by Ghajar et al. (2010a) is extended over to much smoother Nickel tubes.

Second part of the thesis deals with the roughness features which are attached to the walls of microtubes. Nikuradse (1933) performed experiments on tubes with diameters ranging from 2.42 cm to 9.92 cm. Experiments concentrated on the turbulent part of the flow, it was concluded that there is no roughness effect in laminar region. Conclusion was contrary to the plots represented by Nikuradse (1933) in which the points set above the theoretical laminar line. This conclusion suggested that no effect of roughness in laminar region is questionable which was generally ignored by most of the researchers. Kandlikar (2005) investigated Nikuradse (1933) experiments, and the experiments done by the researchers in late 1980's and 1990's. It was concluded by the author that negligence of experimental uncertainties and flow parameters by the researchers, led them to conclude that liquid flows in smooth micro tubes/channels follows along the theoretical lines. It is clear from the discussion above that role of roughness and processes effecting in laminar flow is not clear yet. Looking at the fluid flow through micro tubes/channels, fluid encounters the leading roughness elements and skims over a pocket of circulating fluid before passing over the next element. Based on the above explained phenomenon Kandlikar et al. (2005) proposed constricted parameters, in which flow area was considered to be equal to free flow area. This improvisation resulted negating roughness projection, and in better prediction of friction factor in laminar region.

Above idea was applied to the old stainless steel data by Ghajar et al. (2010a), newly obtained nickel tubes data and on the glass tube data acquired from Ghajar et al. (2010b) conducted at the

University of Macau, China. Available data sets ranged from 0 to 4% relative roughness with few tubes showing rough behavior in laminar region. The constricted parameters suggested by Kandlikar et al. (2005) were used on the available data sets to better predict the laminar region for tubes showing rough behavior in this region. In addition Brackbill and Kandlikar (2007) developed using the constricted parameters a set of correlations to predict the critical Reynolds number. Only micro size channels friction factor were used in developing the correlations by the authors. Proposed correlations are discussed in upcoming chapter, and are employed on the data sets available to test the correlation with micro tubes. If any disagreements are found, improvements will be advised for use of correlation on micro tubes.

CHAPTER III

EXPERIMENTAL SETUP & METHODOLOGY

Effective experimental setup and instrumentation is very important in reducing the experimental uncertainties and measurement errors. As it was observed that in past there have been wide disparity in the results obtained by the researchers for which accuracy of the data obtained from the setup used can be questioned. This chapter discusses in detail the experimental setup involved in taking the pressure drop measurement for the friction factor calculations. This chapter also discusses the constricted flow parameters proposed by Kandlikar et al. (2005) which are used to study flow behavior in laminar region in a better way. Starting with experimental setup it was built by Wendell L. Cook and Clement C. Tang guided by Dr. Afshin Ghajar. The setup is fairly simple to operate but at same time very effective in obtaining the results required. The setup is also very flexible in nature considering the use of different diameters of tubes and testing assembly. The experimental setup consisted of four major parts: (1st) fluid delivery system, (2nd) fluid flow measurement system, (3rd) test section assembly and (4th) data acquisition system.

Schematic of the experimental set up is shown in Fig. 1 and details are discussed subsequently. It is an open loop system, test fluid leaving the test section is collected in sealed container and reused for the experiment.

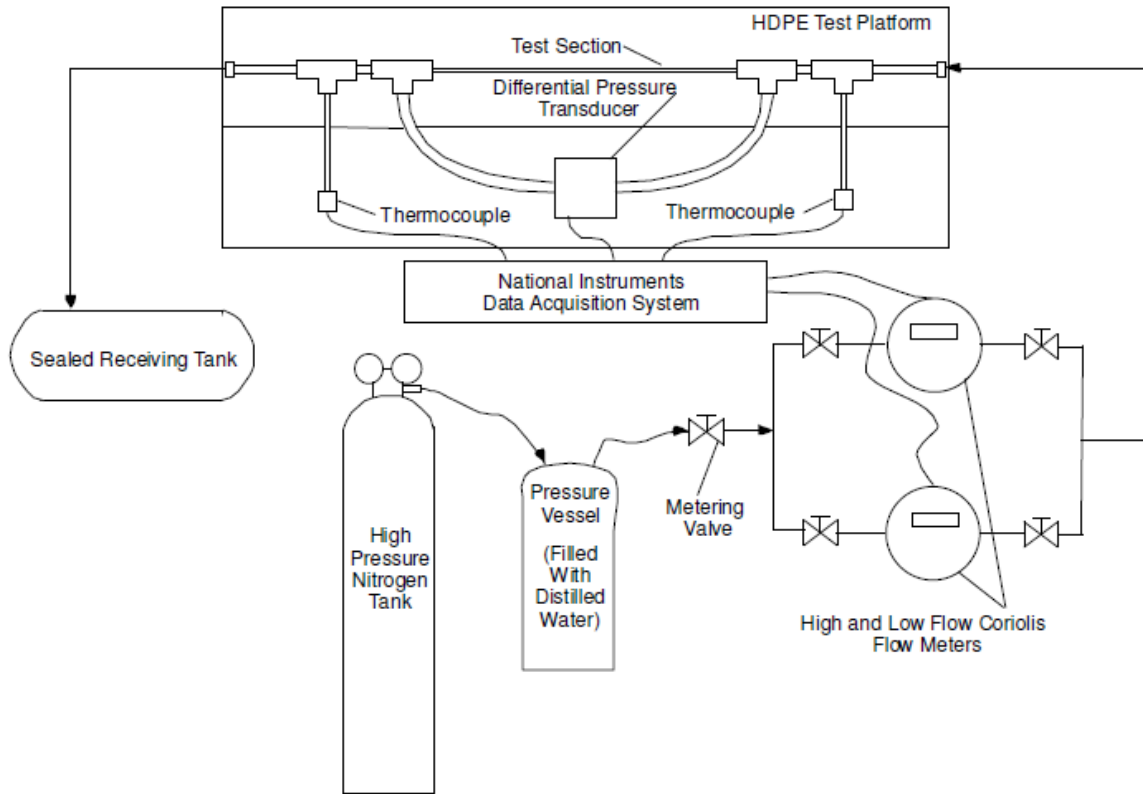


Figure 1: Schematic of experimental setup

3.1 Details of the Experimental Setup

- Fluid delivery system

Fluid delivery system used for this setup was pneumatically pressurized consisting of high pressure nitrogen cylinder (2500 psi) which gives pressure to water as required in the system, being mentioned earlier system being an open loop the fluid after it exits the setup is collected in a sealed container and refilled manually. Nitrogen is forced into a pressure vessel by help of a

dual-stage regulator, pressure vessel is of stainless steel containing the distilled water for experiment. Nitrogen is forced into the pressure vessel from the bottom leading water to push up in a vertical pipe which directs the water flow towards flow measurement assembly before passing through the test section.

Dual stage regulator installed on the pressure tank can deliver the pressure up to 250 psi, to the stainless steel pressure vessel (Alloy products Model no. 72-05) of capacity 5 Gallon (19 Liters). This pressure vessel works on a maximum pressure of 200 psi due to this maximum pressure drop achievable for the test section has limitation of 200 psi. After passing through the pressure vessel water flows through a 1/4inch Omegalex PFA chemical tubing leading to the metering valve (Parker N-Series Model 6A-NIL-NE-SS-V) which controls the amount of water flow into flow meter. Metering valve helps in adjusting the flow according to the Reynolds number required for the flow which is not achievable through the dual stage regulator. Flow meter arrangement has two types of mass flow meters in it. Having two types of flow meters one meter is for high flow and one is for low flow, specifications are discussed under the heading fluid flow measurement system next. After passing through flow meter arrangement water again passes through Omegalex PFA chemical tubing exiting the flow meter arrangement and entering the test section assembly and then exiting the whole setup and gets collected in a sealed container for reuse.

- Fluid flow measurement system

High flow meter is CMF025 coupled with 1700 transmitter, and designed to measure mass flows ranging from 119 lbm/hr (54 kg/hr) to 4806 lbm/hr (2180 kg/hr) with accuracy of 0.05%. Low flow meter is Micro Motion Model LMF3M, coupled with LFT transmitter, measures flows

ranging from 0.00221 lbm/hr (0.001 kg/hr) to 3.3071 lbm/hr (1.5 kg/hr). Flow to the meters is controlled by a dual line setup in combination with ¼ turn ball valves. Two different types of flow meter is used to accommodate all the flow rates required with highest accuracy possible.

- Test section assembly

Test section assembly comprises of five parts-

- I) Test section platform – It is constructed of ½ inch (1.27cm) thick high density polyethylene sheet. This material is very easy to machine for making grooves necessary to fit the tubes, at the same time very durable. Tubes were fitted in the grooves with the help of Super Glue. Parker stainless steel reducing compression fittings of size 1/16 inch (1.59 mm) is used to size down the test section assembly with the test section platform.
- II) Polyimide ferrules – Tubes are tightened with the help of polyimide ferrules made of graphite supplied by Small Parts Inc. These ferrules act as a reducing fitting and bridge the gap between Parker stainless steel reducing compression fitting of size 1/16 inch and the tube.
- III) Tubes – Tubes used for the experiment are Nickel tubes provided by VICI Valco Instruments. Tubes are made by electroformed Nickel meaning Electrolytically cut and polished providing a finish of 1-2 micro inch (0.0254µm). Four different Nickel tubes were used for the experiments 1016µm, 762µm, 508µm and 381µm inner diameter. Length of tubes used for the experiment were 6 inches except for the 1016µm. For this diameter to achieve fully developed condition 12 inch length was necessary, test section platform length can be changed according to the tube length.

- IV) Pressure Transducer – Validyne model DP15 pressure transducer is used for collecting the required pressure drop measurements. Different diaphragms for different ranges of pressure can be tailored in the pressure transducer according to the need, for accurate data and covering the complete range from turbulent to laminar different diaphragms are very necessary. Diaphragms available in the research facility ranged from 0.08 to 200 psi (0.551-1397kPa). Validyne pressure transducer has an accuracy of $\pm 0.25\%$ using full scale of diaphragm. Pressure transducer was connected to the test section assembly by Parker stainless-steel compression tees and 1/4inch (0.635cm) OD PFA tubing.
- V) Thermocouples – Two thermocouples of Omega model number TMQSS-020U-6 are deployed in test section assembly at two spots one at the start of the test section and one at the end of it. Even though the whole test section is isothermal in nature but thermocouples are installed to check for the unexpected heat addition such as frictional heating or heat from outer source. Thermocouples are ungrounded with a length of 6 inch and a diameter of 0.02 inch (0.508 mm), have an accuracy of $\pm 0.5^{\circ}\text{C}$ (0.9°F). Thermocouples are inserted in the flow by the use of two Parker stainless steel compression tees, while maintaining the required sealing.

- Data Acquisition System

Data assimilated by the pressure transducer and thermocouples are in National Instruments Data acquisitions system and recorded in a laboratory computer with installed LabView software.

Data acquisition system has three major parts in its structure:

- Chassis –The chassis is the rack mounted with SCXI 1001. Chassis basic function is to provide a shielded enclosure with forced air cooling and USB connection to the laboratory PC.
- Input Module – module used is SCXI 1102, which is connected directly with the chassis and performs the operation of signal conditioning and functions as a port of connection for the terminal blocks. The above mentioned module has thermocouple input with 32 input channels, receives input from thermocouple as well as mili volt, volt and current. Maximum sampling rate for the received input is 333,000 samples per second.
- Terminal Block – As mentioned earlier input module acts as port of connection for terminal blocks, so terminal block act as an input module for thermocouples. Terminal block used is SCXI 1303. It is a 32 channel terminal block isothermal construction minimizing the error due to temperature differences between the terminals and the cold junction sensor, giving high accuracy thermocouple measurements. Also this terminal block provides automatic ground referencing for the ungrounded thermocouples used in the set up.

3.2 Calibration

For any experimental setup to give accurate measurement calibrating the instruments is the most important task. Experimental setup used in this research has three very important components, which require checking for calibration, they are Omega thermocouple probes, Micro Motion Coriolis and Validyne pressure transducer. Of the three, Validyne pressure transducer needs special attention with reference to calibration because diaphragms are changed frequently

requiring the transducer to be re-calibrated. It also becomes important because erroneous reading with pressure drop will lead to bad friction factor calculations.

Six pressure diaphragms ranging from 8-200 psi were used for capturing the complete range of pressure drops. These diaphragms were calibrated by comparing the voltage output of the differential pressure transducer when applied different pressure with four research grade test gauges. Calibration is performed every time before starting the experiment and when the diaphragm is changed.

Calibration procedure

Illustrated below are the stepwise procedures for calibrating the Validyne pressure transducer.

- Appropriate diaphragm is chosen according to the need of the experiment, starting with the largest range.
- Settle the diaphragm inside the Validyne pressure transducer and check for the two O-rings, that they are not displaced from their position.
- Tighten up all the screws so that there is no leakage when pressurized.
- Connect the positive port of the transducer with the calibration pump.
- Other end of calibration pump is connected to the research grade test gauge.
- Make sure pressure transducer is connected to carrier demodulator and is turned on, carrier modulator's job is to pass the signals to the data acquisition system where the job of evaluation between voltages to the pressure applied is done.
- Tighten all the nuts connecting the pressure transducer with pump, and check for any leakages.

- Bleed all the entrapped air in the pump, and check for the reading of the gauge to be zero before the pumping is started.
- Open up the module on laboratory computer stating as DPS -15 calibration
- Save the module file at appropriate location.
- Assign a name to the file, and now we are ready to record the data.
- Adjust span in the carrier demodulator, such that at maximum pressure of the diaphragm, maximum voltage achieved is 10 Volt or less than that. Maximum voltage should not exceed 10 Volt.
- Record the first point at zero psi for calibration.
- After recording zero psi, make increments of same size let's say 10 psi assuming calibrating 50 psi diaphragm, pump the air and record at each and every increment.
- Now when recording for each and every increment observe the pressure gauge needle that it is at the exact point where it's supposed to be, if required make fine adjustment by the adjustment knob on the pump.
- After following the above mentioned for each and every increment, record the voltage at that increment.
- Once all the points are recorded, a graph is plotted between voltage versus pressure.
- From the graph obtain the trend line equation for the graph which is the calibration equation desired, check for the correlation coefficient R^2 value that either it is 1 or close to 1. R^2 is one way of ascertaining that the calibration equation obtained is accurate. If R^2 value is less than 0.99 redo the calibration.

This completes calibration of Validyne pressure transducer. Figures 2, 3 & 4 show plot of pressure versus voltage for 125, 80 and 50 psi diaphragms along with their calibration equation

and R^2 value. Calibration of 125 psi has total 6 points with an increment of 25 psi. Opening the obtained file from LabView in Microsoft excel and adding the trend line to the points gives the calibration equation. This calibration equation obtained is substituted in the LabView module which records the data from pressure transducer and thermocouple and it governs how pressure transducer is going to perform.

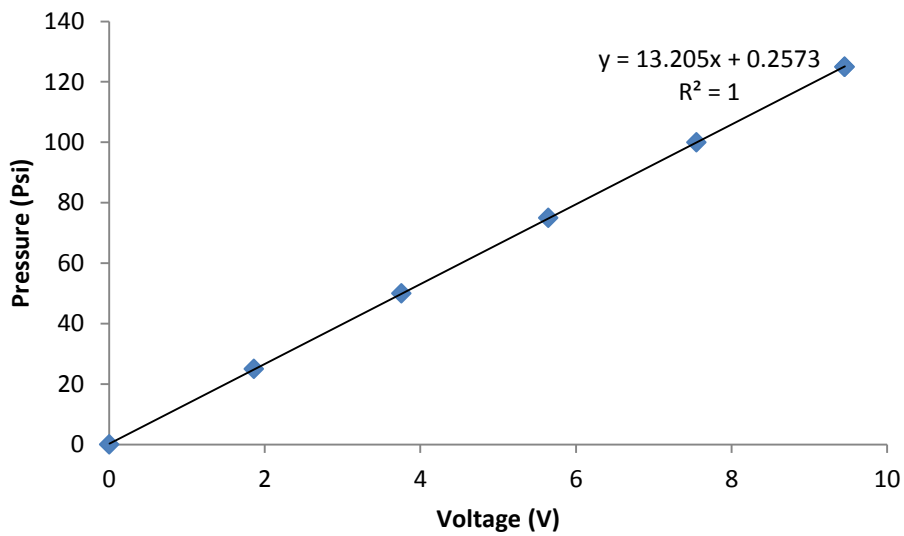


Figure 2: Calibration curve for 125 psi diaphragm

It is very important to check for calibration coefficient R^2 value, it should be 1 or around 1, anything less than 0.99 is not acceptable and recalibration is required.

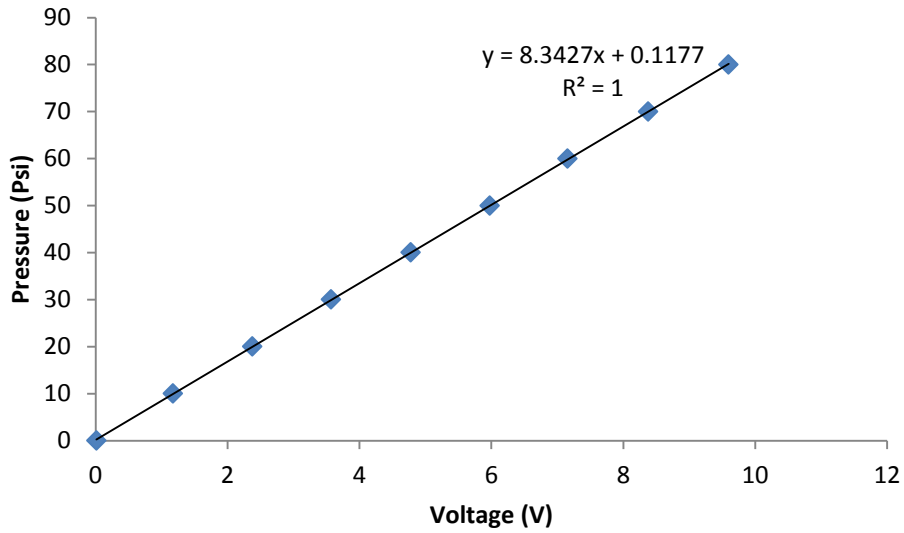


Figure 3: Calibration curve for 80 psi diaphragm

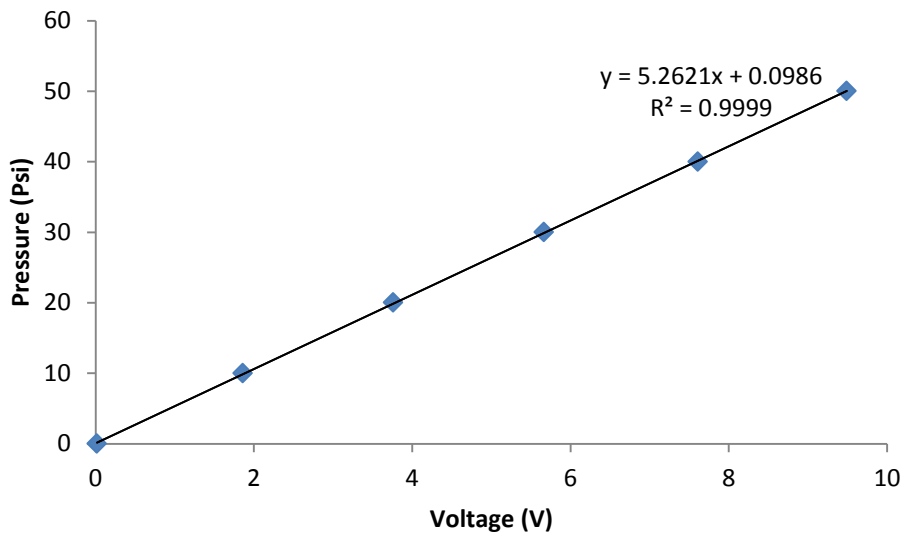


Figure 4: Calibration curve for 50 psi diaphragm

Omega thermocouple probes are factory calibrated with accuracy of $\pm 0.9^\circ\text{F}$ ($\pm 0.5^\circ\text{C}$). In this set up experiment is done with relatively constant temperature so it is not required to calibrate the

thermocouples extensively like pressure transducer. To validate the factory calibration of the thermocouple probes, they were compared against a known water temperature.

Micro Motion Coriolis flow meter was factory calibrated as well. For CMF -025 manufacturer's specified tolerance for calibration error is $\pm 0.1\%$. For LMF3M, manufacturer's calibration tolerance is $\pm 1.0\%$. To check with the manufacturer's calibration in lab was timed collection of water flowing through the flow meter at certain flow rate. Also in addition the maximum and minimum milliamp outputs of the CMF-025 were fine-tuned so that flow rate seen by the meter in laboratory conditions enhanced.

3.3 Experimental Procedure

Illustrated below are the step wise procedures for running successful experiments.

- Connect the Validyne pressure transducer with the appropriate calibrated diaphragm affixed in it, starting with largest range diaphragm.
- Check the connection's near the pressurized water tank and near the test section for the loose connection if any that might cause leakages.
- Fill in the pressurized water tank with water.
- Check for valves (hi flow & low flow) of the flow meter that the desired valve is open and the undesired valve is closed.
- Turn on the mass flow meter and wait for the status light to turn from red to yellow to green and reading as 0.0 kg/min
- Open the valve on the nitrogen cylinder completely, which has a two phase regulator and line.

- Maneuver the Airgas regulator on the nitrogen cylinder so that the required amount of nitrogen gas is filled in the pressurized water tank.
- Make sure that all the valves are closed on the pressurized tank and wait for a minute or two so that the pressure builds up properly in the tank.
- Open LabView module, run the software and navigate to the folder where data is required to be saved.
- Name the folder according to the tube's diameter.
- Open the valve on the pressurized water tank, open the metering valve completely so that the flow is directed towards flow meter and further in the line.
- Due to sudden opening of the valve on the pressurized vessel there's a small difference in pressure generated due to time elapsed for pressure in cylinder to stabilize the pressure in the vessel.
- Wait for 4-5 minutes for the system to stabilize without recording any data, giving time for the pressure to build up and stabilize in both cylinders.
- Next step is to bleed the air out of the flow meter before sending the water through the test section because the flow meter may contain some air which can give unwanted bubbles in the test section leading to the bad pressure drop readings. To bleed the air out of the flow meter open a small bleeder at the of exit line of flow meter.
- Similar bleeding is required on the Validyne pressure transducer, it is done by bleeder provided on both side of the transducer.
- Wait again 2-3 minutes for system to stabilize, after bleeding it can be seen there is a difference between what the gauge is reading now.

- If the reading is stable on the gauge in the flow meter, start recording the data by clicking the record button on the LabView screen.
- Record the data for each Reynolds number for 30 seconds. To change to different Reynolds numbers adjust the metering valve to change the flow rate, keeping the pressure in the vessel unbothered.
- Before recording the data at each point, after adjusting the metering valve wait again till the time that reading on the gauge is constant.
- Keep in check the amount of water left in the pressurized water tank by observing the amount of water collected. Completely empty water tank should be avoided because it will fill the line with air which is not desired.
- As the water in the vessel is about to run out turn off the valve on the pressure vessel, turn off the nitrogen gas tank.
- Release the nitrogen trapped in tank by opening the release valve. Open water tank refill with the water collected in the sealed collecting chamber. Start the system again as described above.
- Once the experiment for the day is completed exit LabView switch off the set up, release the pressure from water tank and turn off the nitrogen tank.

3.4 Experimental Uncertainties

Every experimental work has some uncertainties always attached to it and this section of the report will be incomplete if it is not discussed here. To understand the uncertainties in the

friction factor data presented, it is to be noted that Darcy equation (Eq.1) has been used to calculate the experimental friction factor values.

$$f = \frac{2\Delta p D}{\rho L V^2} \quad (1)$$

Looking at velocity term in (Eq.1) velocity is calculated from mass flow rate equation which contains area term in it (Eq.2) which is rearranged as shown in (Eq.3)

$$\dot{m} = \rho A V \quad (2)$$

$$V = \frac{\dot{m}}{\rho A} \quad (3)$$

Where area is given by (Eq.4)

$$A = \frac{\pi D^2}{4} \quad (4)$$

Therefore

$$V = \frac{2\Delta p D^5 \rho \pi^2}{16 L \dot{m}^2} \quad (5)$$

Substituting this value of 'V' in (Eq.1) we get equation for friction factor as (Eq.6)

$$f = \frac{2\Delta P D^5 \rho \pi^2}{16 L \dot{m}^2} \quad (6)$$

From the above equation (Eq.6) it is observed that there are five different variables upon which the uncertainty in calculation of friction factor depends. These are (1) Pressure drop, (2) Tube inner diameter, (3) Density, (4) Tube length and (5) Mass flow rate. Looking at uncertainties by each factor discretely it should be noted that pressure drop, tube length and mass flow rate can be controlled in the laboratory. Density of water is assumed to be constant as the temperature in the

laboratory room is controlled. Tube inner diameter uncertainty depends upon the manufacturers specifications and manufacturing accuracy, tube inner diameter does not represent the accuracy of experimental setup. However Scanning Electron Microscopy is used to ensure and measure tube inner diameter. In the next few paragraphs each uncertainty factors will be discussed in detail.

First looking at pressure drop uncertainty, pressure drop is obtained by using Validyne pressure transducer and as mentioned earlier specification of the transducer is $\pm 0.25\%$ of the full scale reading of each diaphragm used. To further reduce the uncertainty, diaphragms were carefully selected in order to obtain the highest accuracy possible and covering the maximum range. To confirm the accuracy of the diaphragm, over lapping the lower end of one diaphragm with upper end of the next diaphragm was made mandatory. Even though after taking such attention worst situation occurs with small tubes and low Reynolds number, and estimation of uncertainty in this situation is important. For this situation uncertainty in the pressure drop measurement was found to be $\pm 1\%$ of reading refer Ghajar et al. (2010a). Looking at the intermediate sized tubes and flow rates, uncertainty in pressure drop measurement is $\pm 0.4\%$ of reading when pressure transducer is pushed to its limits.

Mass flow rate is measured by Micro Motion Flow meter specification for high flow meter CMF-025 meter is $\pm 0.5\%$ of reading and it is used for high flows and larger tubes, but it should be noted that this flow meter is used for flow ranges lower than its range to cover the entire range of flow rates for the tube under experiment. Low flow meter LMF3M meter specification is $\pm 0.5\%$. Based upon the uncertainty equation provided by the flow meter manufacturers maximum uncertainty between two meters is $\pm 1.8\%$. Thus the above mentioned data helps in determining the uncertainty in mass flow rate.

Tube length uncertainty is determined by the accuracy in cutting the high density polyethylene tube cradles, in which the tube is mounted for experiment. Length of the cradle serves as reference for mounting the tube sections ensuring consistency in tube length. Measured uncertainty in the cradle lengths is $\pm 0.26\%$ of length.

Three different uncertainty values have been established till now. In order to estimate overall uncertainty, an analysis was conducted using the Kline and McClintock (1953) method for estimation of overall uncertainty. For larger tube sizes and high Reynolds numbers, the CMF-025 meter is used and is functioning at the manufacturers specified uncertainty level. The pressure transducer is operating at the better of its two calculated uncertainty levels. Taking this into consideration, the overall uncertainty is calculated at $\pm 0.83\%$. For small tube size and low Reynolds number, the CMF-025 meter begins to operate under range. In this area, the pressure transducer is considered to be operating at the lesser of its two uncertainty levels. In this range, the overall uncertainty associated with the experimental apparatus is calculated at $\pm 2.78\%$. Finally, for the lowest ranges of tube size and Reynolds number, the LMF3M meter is used, the pressure transducer is still operating at the lesser of its two uncertainty levels. For this lowest Reynolds number and smallest tube size situation, the overall uncertainty decreases to $\pm 1.51\%$.

Diameter Measurement

Tube inner diameter is one factor for uncertainty, which cannot be controlled in laboratory as it is not manufactured in the laboratory, purchased from outside source so have to be on their mercy in precision of machining the tube. However what can be done in the laboratory is cross checking the specification provided by the manufacturer. For that purpose to check the specified tube inner diameter Scanning Electron Microscope (SEM) at Oklahoma State University

microscopy lab was utilized. Tube selected for this examination was (0.030 inch) 762 μm . Imaging was done using JEOL JXM 6400 Scanning Electron Microscope System in combination with a digital camera, resolution of the microscope ranged from 30-50 nm. After capturing the image based on the scale of the picture, the inner diameter of the tube was estimated by measuring the image pixels. It was found that the estimated tube diameter was within $\pm 2.62\%$ of the specified diameter, which was within $\pm 3.33\%$ of the manufacturer's specification. Example of image is shown in Fig. 5. . Image was captured from top, and the sample was kept at an angle of 90° with the surface.

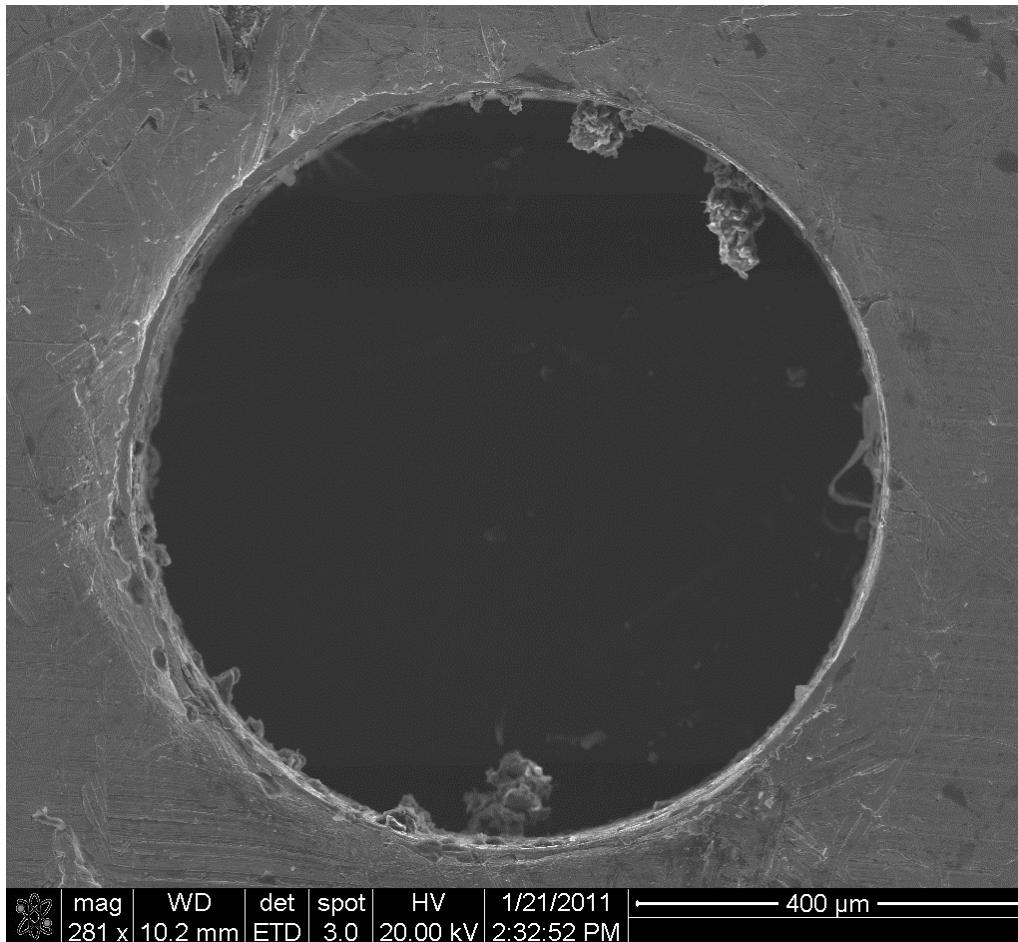


Figure 5: SEM image of $762\pm 25\ \mu\text{m}$ (manufacturer's specification) diameter Nickel tube. Based on this SEM image tube diameter was found to be $782\ \mu\text{m}$.

3.5 Constricted Flow Parameters

In all the studies performed on microtubes for friction factor calculation tube inner diameter was taken directly into calculations. Recently Kandlikar et al. (2005) proposed a new way of looking at the diameter based on constricted flow parameters. This part of chapter reviews the constricted parameters and the new equation proposed for calculation of friction factor, explaining constricted parameters and how the new friction factor equation evolves out of it. Equation is later used on different data sets.

Starting with defining constricted parameters, a microtube has a diameter d but with roughness all around the inner walls of tube, parameter $D_{h,cf}$ represents new constricted diameter. ϵ_{FP} is roughness element height based on proposed constricted parameters. The parameters can be understood better by referring to Fig. 6.

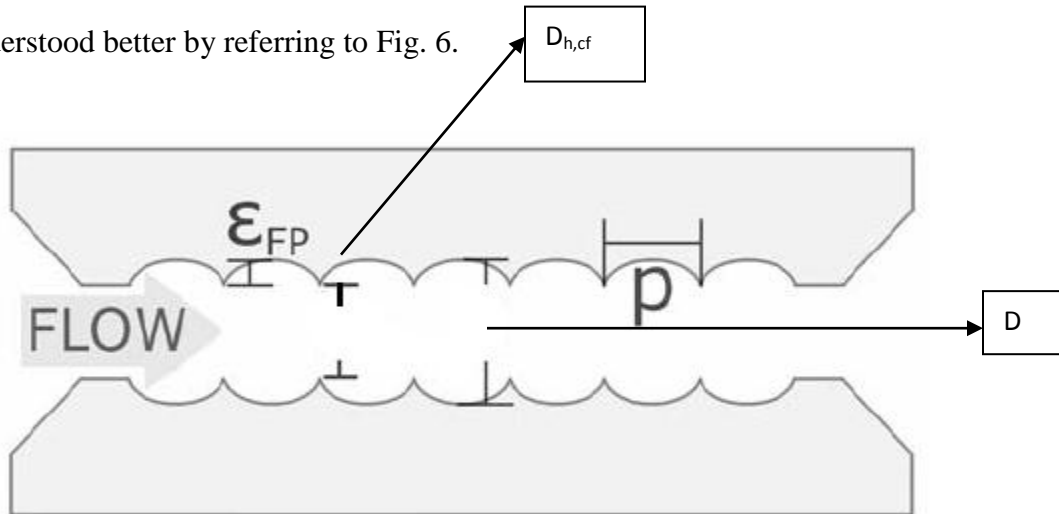


Figure 6: Side view of microtube with parameters marked (Kandlikar et al. 2005).

The curved surface represents the roughness profile. It is assumed to be even throughout the tube even though it might not be the case in practice. It should be noted that pitch p , of roughness

element does not play a large role in the uniform roughness assumed for the development of constricted flow equations.

To calculate new constricted parameters $D_{h,cf}$, A_{cf} and P_{cf} are defined as follows

$$D_{h,cf} = D - 2\varepsilon_{fp} \quad (7)$$

$$A_{cf} = \frac{\pi D_{cf}^2}{4} \quad (8)$$

$$P_{cf} = \pi D_{cf} \quad (9)$$

Based on the parameters defined above, equation for constricted flow friction factor proposed by Kandlikar et al. (2005) is given by Eq. (10).

$$f_{cf} = \frac{f D_{cf} A_{cf}^2}{D A^2} \quad (10)$$

Constricted Reynolds number is calculated by using Eq. (11)

$$Re_{cf} = \frac{4\dot{m}}{\mu P_{cf}} \quad (11)$$

A major purpose of using the constricted parameters proposed by Kandlikar et al. (2005) is that it effectively predicts the friction factor for laminar region. This method steers back the friction factor value for laminar region back to theoretical laminar line therefore, reducing the roughness effect in laminar region. Using the friction factor and Reynolds number Equations (10) and (11), Brackbill & Kandlikar (2007) proposed two correlations. It was recommended that use of these

correlations provides a method for prediction of the critical constricted Reynolds number, for not so smooth tubes to the point of smooth channels of similar geometric parameters.

$$0 < \frac{\varepsilon}{D_{h,cf}} \leq 0.08 \quad Re_{c,cf} = Re_o - \frac{Re_o - 800}{0.08} (\varepsilon/D_{h,cf}) \quad (12)$$

$$0.08 < \frac{\varepsilon}{D_{h,cf}} \leq 0.15 \quad Re_{c,cf} = 800 - 3270 (\varepsilon/D_{h,cf} - 0.08) \quad (13)$$

where $Re_o = 2500$ which is transition for $\varepsilon/D_{h,cf} = 0$.

These correlations were developed based on the critical Reynolds number obtained by using Equation (11) and constricted relative roughness $\varepsilon/D_{h,cf}$. It was observed that increasing relative roughness yields lower critical Reynolds number. This trend is presented by the authors as shown in Figure 7. Lines are the best fits for data presented by Brackbill & Kandlikar (2007) and represent the correlations proposed by the authors.

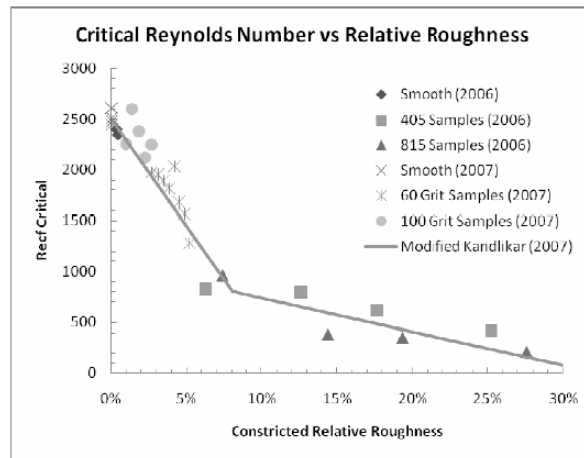


Figure 7: Critical Reynolds number with constricted relative roughness, lines representing correlations (12) & (13) (Brackbill & Kandlikar 2007)

In present work analysis was performed on first correlation [Equation (12)] only as the experimental data available is up to $\varepsilon/D_{h,cf}$ of 0.043. The friction factor equation was used to calculate new friction factor for the laminar region for nickel tubes, previous stainless steel tubes data and glass tube data obtained from Macau China.

CHAPTER IV

RESULTS & DISCUSSION

From the review of previous work few points are distinctly pointed out. It is clear that great amount of work is still required to better understand the flow behavior through microtubes. As most of the authors found disparities in the results of friction factor regimes in microtubes. Tube diameters, surface roughness were remarked as the prominent reasons for disparities in results observed. This point to the direction that extensive research with varied tubes of different diameter and roughness. It should be noted that till now materials used for experiments were steel, fused silica and glass more or less with different relative roughness. The roughness was obtained typically by etching, with this method consistency of roughness elements throughout the length of the tube/channel is questionable. At this point it becomes important to perform experiments on tubes/channels of varied materials, and procured directly from the manufactures. Tubes/channels which are manufactured/drawn using different machining procedures are more consistent in fabricating roughness elements. Eventually this will help in getting better results. Subsequently next most important factor is careful measurement of pressure drop data. As discussed in the previous chapter about instrumentations and uncertainties involved with it, selection of pressure sensing diaphragms becomes very important. Appropriate selection of pressure sensing diaphragm is important for clearly detecting the transition regime. Transition

regime as outlined by Ghajar et al. (2010a) is of highest importance, as clearly identifying transition ensures good sensitivity and accuracy with instrumentation and the experiment performed. Good sensitivity and accuracy captures proper start and end of the transition regime.

Laminar regime was one region which has been ignored or in other words conceded as region with no roughness effect. This conjecture was overruled by Kandlikar et al. (2005) based on the authors' experimental findings. It implies that advance research is required to assess the conclusions made by Kandlikar et al. (2005). Transition regime also comes under speculation because of loose effort with laminar region, as change in results of laminar regime possibly will alter the results of transition regime.

4.1 Diaphragm Effects

Diaphragm plays a very crucial role in correct prediction of transition regime, and for proper understanding of roughness in a fluid flow through micro tubes/channel. Each diaphragm has a sensitivity span for that particular range diaphragm. To determine the sensitivity span of an individual diaphragm it is necessary to collect the pressure drop data for the complete range of diaphragm, furthermore accuracy is also improved with this practice. Sensitivity span of a diaphragm is validated by overlapping lower end of larger diaphragm with higher end of the next smaller diaphragm. The part of larger diaphragm which overlaps well with smaller diaphragm is considered to be range of good sensitivity span whereas rest is unreliable. The inconsistent part of higher diaphragm is doubtful for its accuracy in measurement of pressure drop across the tube. Above viewpoints are talked about in Ghajar et al. (2010a), and are directly adopted in the present work to verify and explore new conclusions related to the effects of diaphragms.

In reference to the Ghajar et al. (2010a) Figure 8 elucidates the comparison between various diaphragms and respective pressure sensitivity span for 2083 μm steel tube. Inspecting Figure 8 it is seen that the higher end of 34.5 kPa and 55.2 kPa diaphragm are in well agreement with 138 kPa diaphragm. But 138 kPa diaphragm takes a completely different route after first few points which is not in agreement with next lower 55.2 kPa or 34.5 kPa diaphragms. Similarly for 55.2 kPa diaphragms it is in good agreement with 34.5 kPa diaphragm but starts detaching before 2000 Reynolds number which suggests the effect of roughness. It may not be the case as lower end of 34.5 kPa is validated by next lower diaphragm 13.8 kPa. For further accuracy in laminar range smaller diaphragm 3.45 kPa is used. Similar illustrations were addressed for two other steel tubes by the Ghajar et al. (2010a).

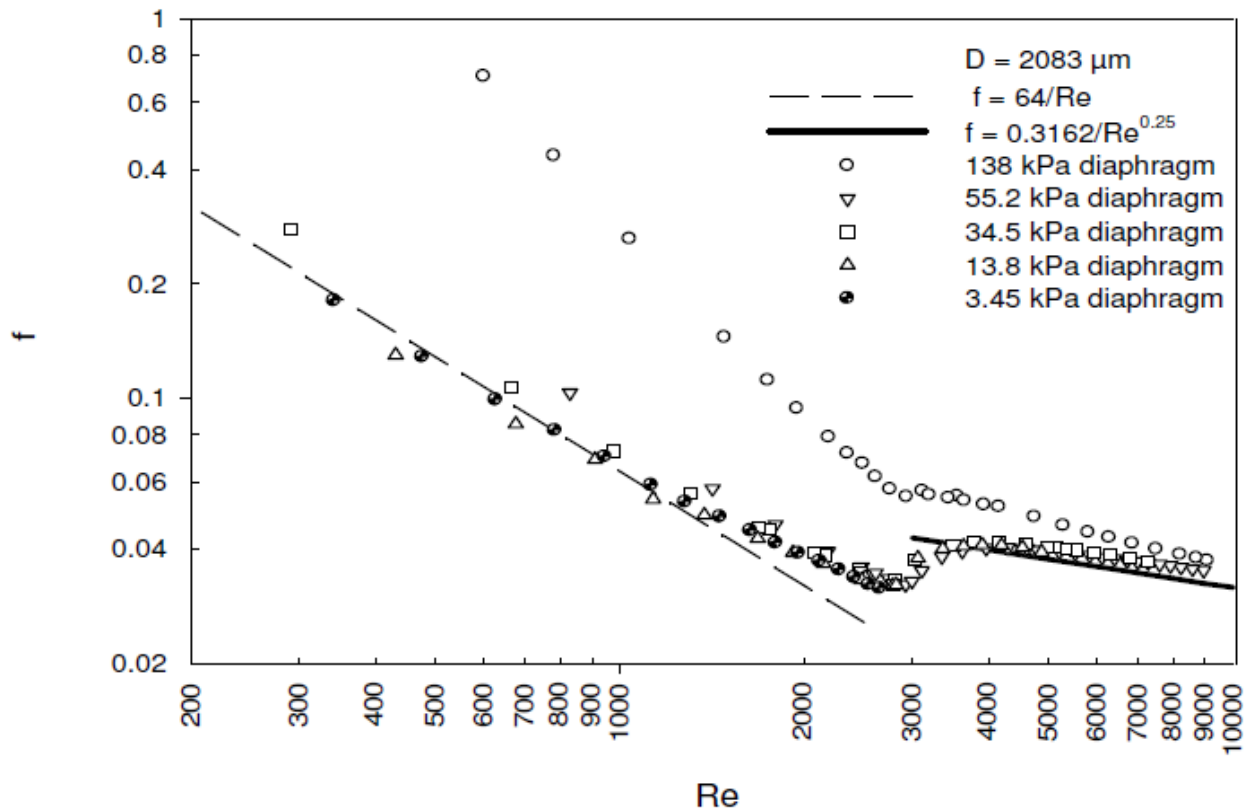


Figure 8: Comparison of various diaphragms for 2083 μm steel tube (Ghajar et al. 2010a)

It is clear from Figure 8 that each diaphragm works for its particular range and if only one diaphragm as in the above case [0-20 psi (138 kPa)] would have been used, results would have been drastically different and wrong. Thus, it can be inferred from the above figure that several diaphragms are required to use for different ranges of flow. Correct flow curve can only be determined by selecting appropriate diaphragm with correct sensitivity for the particular range.

Review of discussion by Ghajar et al. (2010a) on diaphragm effects appears as important at this stage because as we look into diaphragms effects for nickel tubes. The behavior of diaphragm effects is expected as steel tubes, but there is a variation which was unaddressed. Figure 9 shows the various diaphragm behaviors with nickel tube of 762 μm in diameter. It can be observed here that similar shift in curves for different range of diaphragms is observed for nickel tubes. This shift is not as significant as observed in steel tubes (Figure 8) by Ghajar et al. (2010a).

Observing Figure 9 it is clearly visible that 551.5 kPa diaphragm's lower range agrees adequately with the lower range of the next 345 kPa diaphragm. There is a slight variation in the laminar regime of the two diaphragms, as the last few points give a hint that 551.5 kPa will take a different path for laminar region than 345 kPa diaphragm. It could have been more prominently visible but due to experimental constraints additional points in laminar region could not be obtained. The 345 kPa diaphragm is further verified by 137.8 kPa, but as it is visible lower end of 345 kPa starts peeling off after 2000 Reynolds number. It gives a false impression about the surface roughness for this nickel tube. Better transition was predicted by 137.8 kPa diaphragm which was further verified by 55.1 kPa diaphragm.

Looking at the other tube it is clear again that there is no deviant behavior by any diaphragm but there is difference in prediction of laminar friction factor. From the Figure 10, 551.5 kPa and

344.7 kPa falsify the roughness effects in the laminar region. This implies that 861.8 kPa is good for turbulent region and 551.5 kPa and 344.7 kPa are appropriate for $Re > 2300$ whereas 137.8 kPa and 55.1 kPa diaphragms are appropriate for capturing laminar region. Data points obtained by 137.8 kPa are further verified by 55.1 kPa diaphragm.

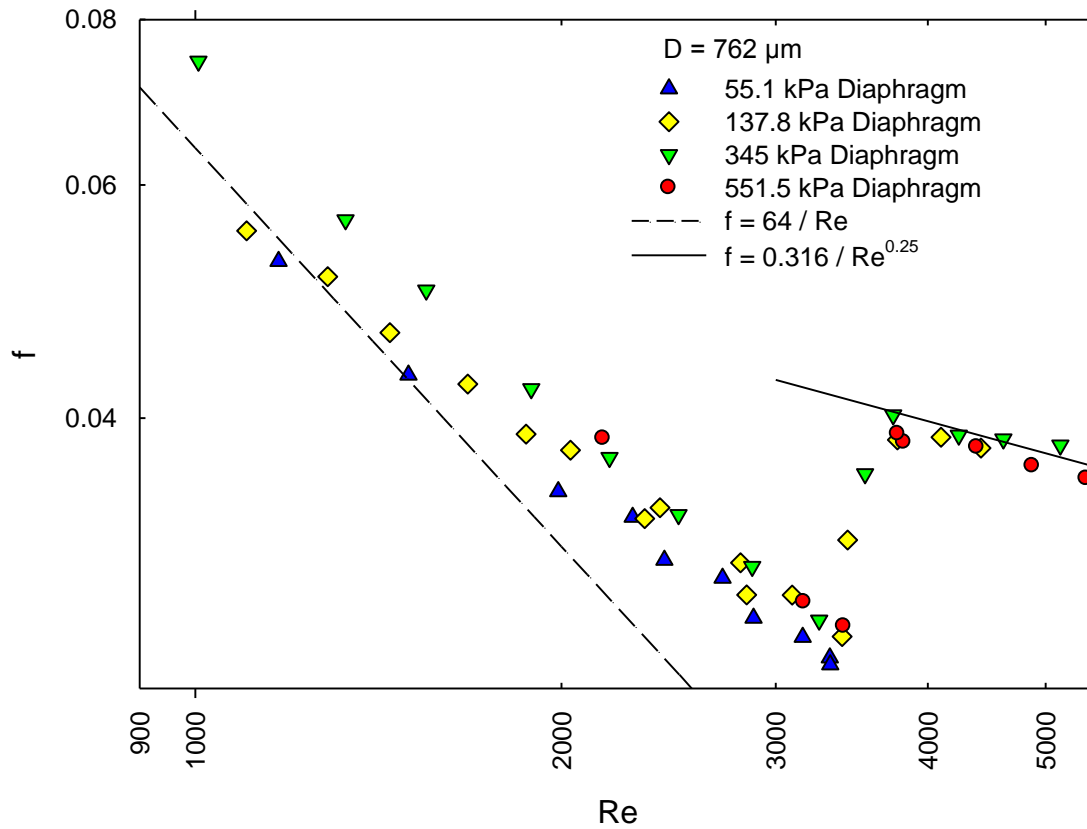


Figure 9: Comparison of various diaphragms for 762 μm nickel tube

Now if we focus on the transition region for diameter 508 μm shown as Figure 11, it is interesting to note that 861.8 kPa, and 551.5 kPa diaphragms are suggesting modest difference in the transition region. The discrepancies in the data points of the above two diaphragms indicate that the transition region was not captured properly. Good transition was measured by 344.7 kPa

and verified by 137.8 kPa diaphragm. Percentage error measured by 551.5 kPa was 7 % higher than 137.8 kPa diaphragm at the trough of the transition region.

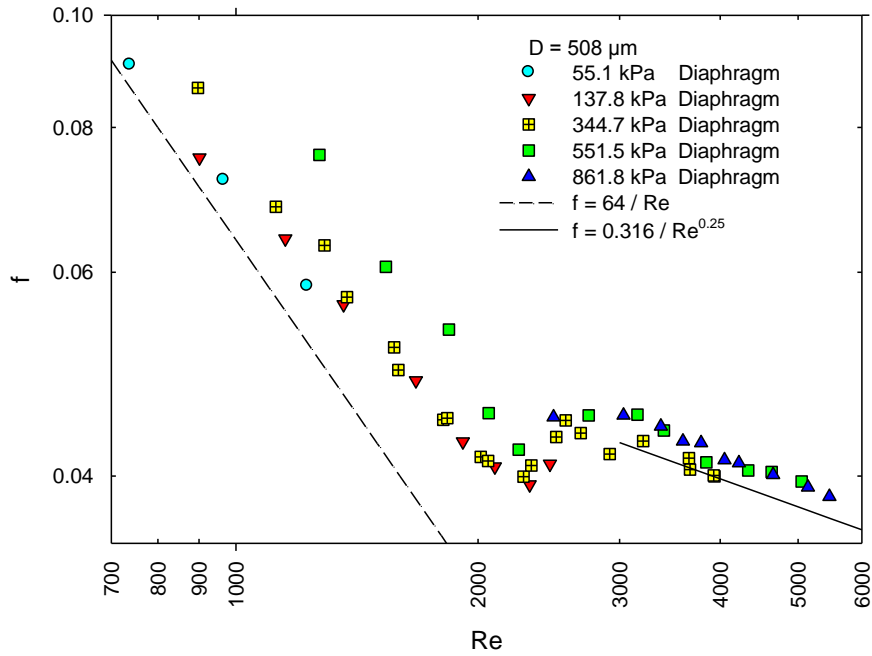


Figure 10: Comparison of various diaphragms for 508 μm nickel tube

From the above discussion correct diaphragms are required to be used for appropriate range of Reynolds number. From Figures 9, 10 and 11 we can establish that use of wrong diaphragm for the particular range will lead to error in measurement of friction factor for that range. Such errors were also observed with two other nickel tubes.

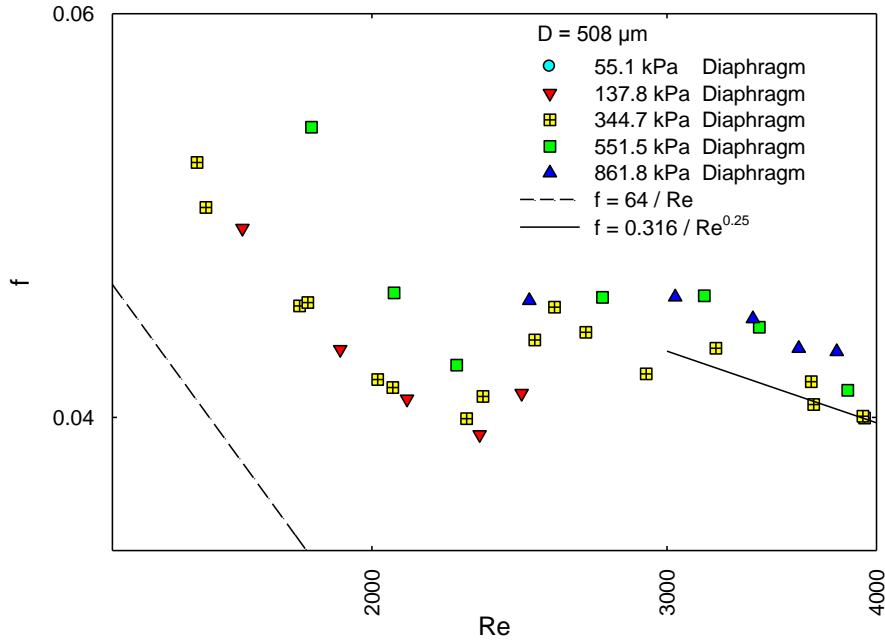


Figure 11: Comparison of various diaphragms with focus on the transition region for 508 μm nickel tube

The reason for this error can be explained using accuracy of the pressure transducer. For the given diaphragm the accuracy was mentioned in Chapter III as $\pm 0.25\%$ of the full scale value. When diaphragm is changed from 861.8 kPa to 55.1 kPa the accuracy improves from 2.15 kPa to 0.137 kPa. The improvement in accuracy is reflected in accuracy of friction factor from Equation (6) given in Chapter III.

4.2 Nickel Tube Results

This section of the chapter demonstrates the results obtained by four different nickel tubes with 1016 μm , 762 μm , 508 μm and 381 μm inner diameters. All the three flow regimes laminar, transition and turbulent were investigated for Reynolds numbers ranging from 400 to 10,000. Experimental laminar region was compared with theoretical friction factor equation given by Poiseuille for fully developed flow in the laminar region $f = 64/\text{Re}$. Experimental friction factor in the turbulent region was assessed with Blasius friction factor equation for turbulent flow i.e. $f = 0.316/\text{Re}^{0.25}$.

Figures 12 to 15 display the four nickel tube results compared with theoretical results of laminar and turbulent regions. It is arranged in descending order of inner tube diameter. Transition region was calculated by finding the Reynolds number at the points where friction factor departs from laminar region and the point where it merges with the turbulent line. The critical Reynolds number was decided when experimental data point deviated from the laminar line by more than 5% as mentioned in Ghajar et al. (2010a). Uncertainties involved in experimental apparatus as mentioned in the previous chapter were $\pm 2.78\%$ but to be on the safe side 5% deviation criteria was used. Based on the above mentioned criteria transition region was understood to have begun when the data point was 5% deviated from the laminar line and ends with data point that is 5% lower than identified turbulent line. Identified turbulent line in the graph is a straight line for $\text{Re} > 4000$ representing the theoretical data points for turbulent region.

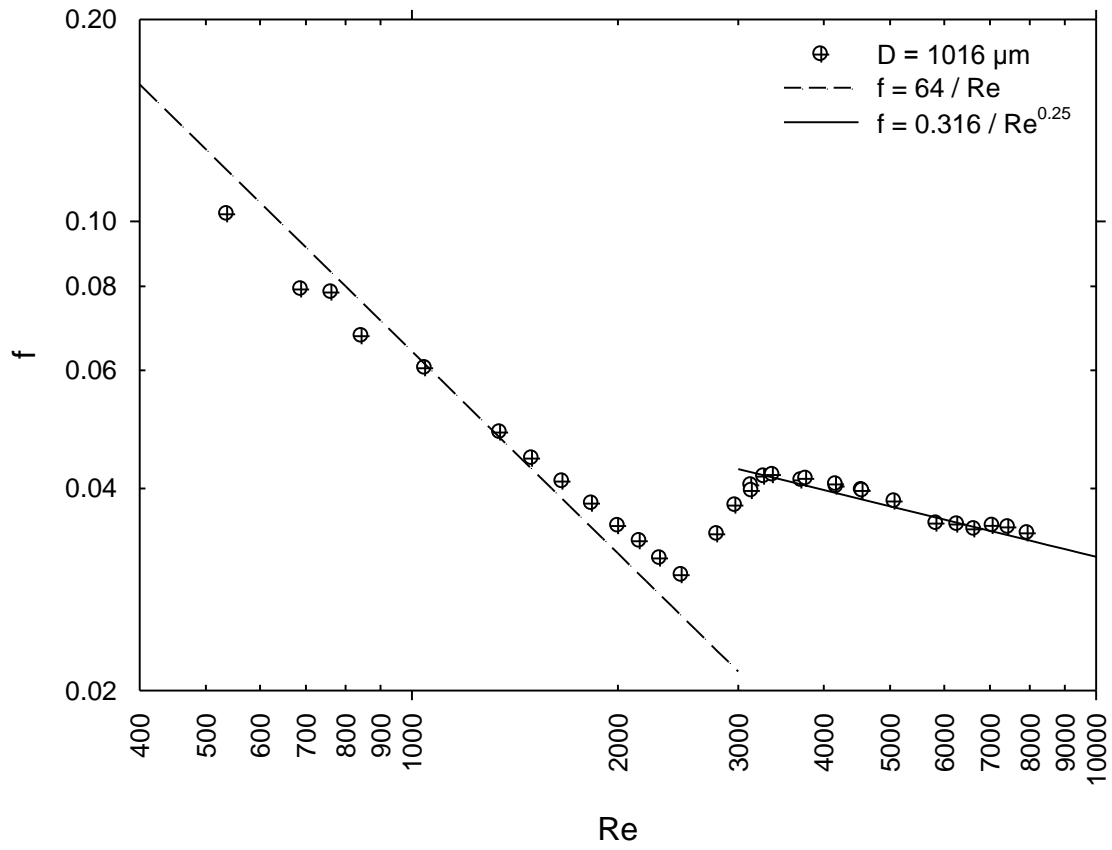


Figure 12: Diameter = 1016 μm transition region ($1650 < Re < 3350$)

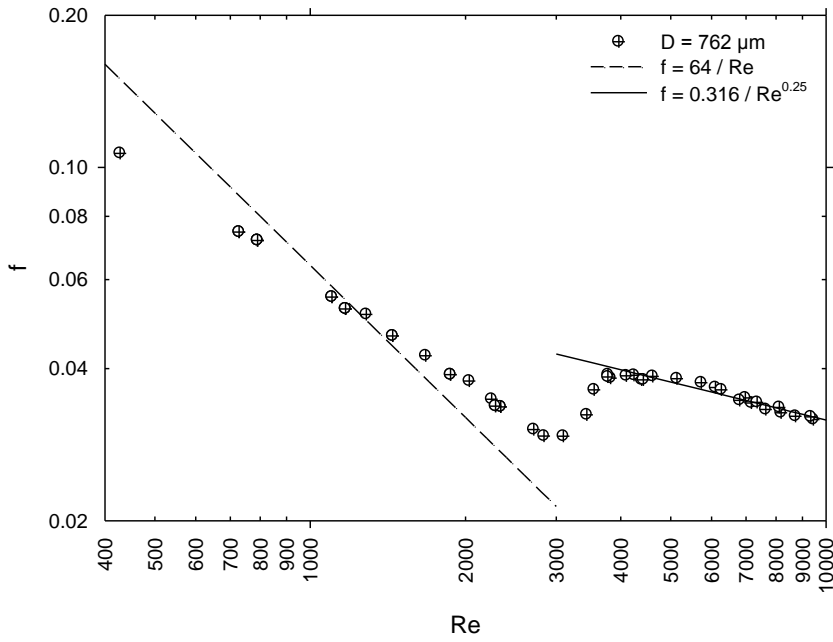


Figure 13: Diameter = 762 μm transition region ($1450 < Re < 3700$)

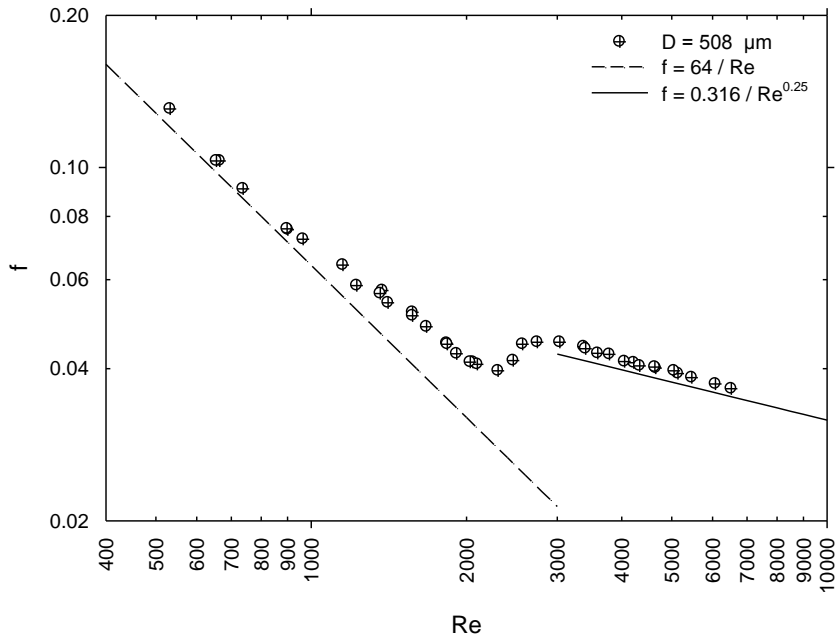


Figure 14: Diameter = 508 μm transition region ($950 < Re < 3300$)

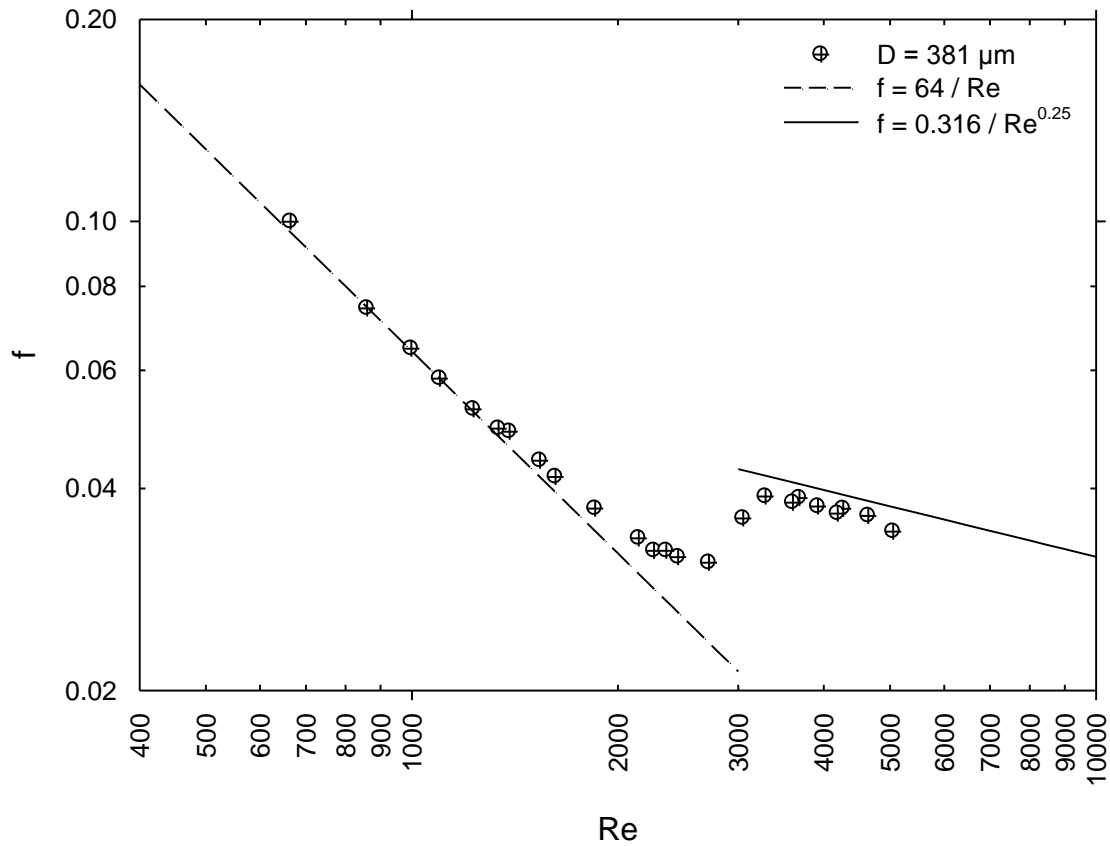


Figure 15: Diameter = 381 μm transition region ($1850 < Re < 3250$)

Detailed study of experimental results of the nickel tubes provided many distinctive behaviors, few points were similar to that observed in the past while some are new in the fragmentary study of the mini/micro channels/tubes. It was observed that predominantly smooth tubes followed the theoretical laminar line. However there was a trend in the laminar region for the three tubes i.e. 1016 μm , 762 μm and 508 μm . Their period of stay in the laminar region was based upon their inner diameter. The 1016 μm tube had the longest laminar regime with flow departing only at 1650 Reynolds number, for the 762 μm tube flow left the laminar line at 1450 Reynolds number and for the 508 μm tube flow deviated from the laminar behavior at 950 Reynolds number. This inspection suggests that there is no delay in transition and critical Reynolds number was

dropping with decrease in the inner tube diameter. However, similar behavior was expected for the 381 μm tube but it was not detected, flow departed the laminar line at 1850 Reynolds number. Thus, flow at laminar region was longest for the tube with smallest inner diameter and consequently delay in transition was observed. Similar nature of delay in transition was seen by Ghajar et al. (2010a), but the authors observed the delays right from the start with decrease in tube diameter. This advocates both conventional theories and unconventional occurrences observed by Ghajar et al. (2010a) and Ghajar et al. (2010b). Unconventional experiences might be stronger if tube diameter was reduced, but experimental constraints did not allow further decreasing the diameter.

Examining the transition region, Table 1 lists transition ranges for all the four nickel tubes. The transition range of the tubes was increasing till the 508 μm tube and then a decrease in transition range was observed for the 381 μm tube. Transition started in between Reynolds numbers 900-1900. Transition ended with Reynolds number roughly 3300, only for the 762 μm tube transition was dragged up till 3700 Reynolds number.

Investigating all the tubes tested, no complete parallel upward shift of friction factor profile from the theoretical line was observed for the tubes. All the tubes were roughly in good agreement with conventional theoretical predictions. Similar observations were made by several investigators (refer to Table 2). It implies that there is no roughness effect. It should be noted that these nickel tubes are very smooth tubes so this behavior was anticipated.

Table 1: Transition range for different nickel tube diameters tested.

| Tube I.D.[μm] | Relative Roughness ϵ/D (%) | Transition Range |
|--|---|-----------------------------------|
| 1016 μm | 0.005 | 1650 < Re < 3350 [See Fig. 12] |
| 762 μm | 0.006 | 1450 < Re < 3700 [See Fig. 13] |
| 508 μm | 0.01 | 950 < Re < 3300 [See Fig. 14] |
| 381 μm | 0.013 | 1850 < Re < 3250 [See Fig.15] |

Figure 16 shows the comparison of all the nickel tubes experimented. An unusual arrangement of friction factor profiles with respect to each other was noticed. At this low relative roughness (0.01% - 0.005%) a specific trend similar to Ghajar et al. (2010a) was not observed. It was seen that the entire curve of tubes did not pile up in either ascending or descending order of tube diameter. In the laminar region 1016 μm , 762 μm and 508 μm tubes had a trend, with tubes placed on top of next larger tubes. Except the 381 μm tube which showed an unexpected behavior. The 381 μm tube was following the laminar line very closely and for an extended period despite being smallest in the group. To confirm the veracity of experimental setup and that there is no fickleness with it, one set of experimental readings were recorded in reverse order of normal practice. Normal practice is recording the data points for particular tube starting with high flow first and then going down with the mass flow rate. To authenticate the tube used for

experiment another tube of the same inner diameter by the same manufacturer was used for the pressure drop runs, identical flow behavior was observed.

Some inconstancy was observed in the transition region as well. There was no particular inclination of region based on the tube diameter. It was expected that friction factor profile will shift upwards with decrement of diameter, as observed by Ghajar et al. (2010a) and shown in Figure 17. The figure is generated using the data provided by Ghajar et al. (2010a) for all their steel tubes. It is very clear from the Figure 17 that as the diameter was reduced friction factor profile shifted upwards.

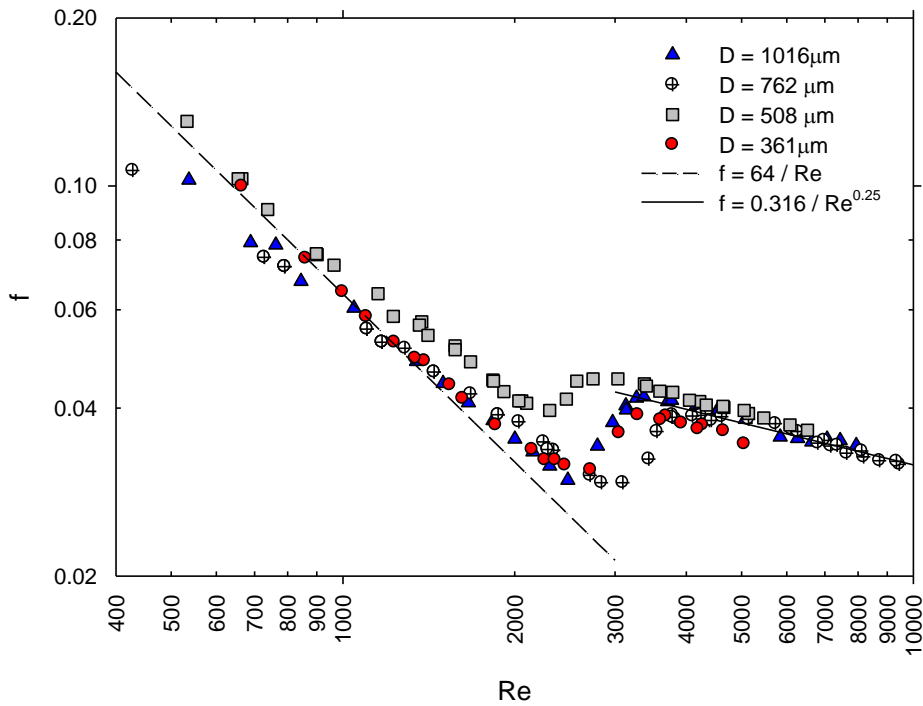


Figure 16: Comparison of experimental data for 1016 μm , 762 μm , 508 μm and 381 μm nickel tubes

For the nickel tubes rather an irregular pattern was observed with respect to friction factor profile in the transition region.

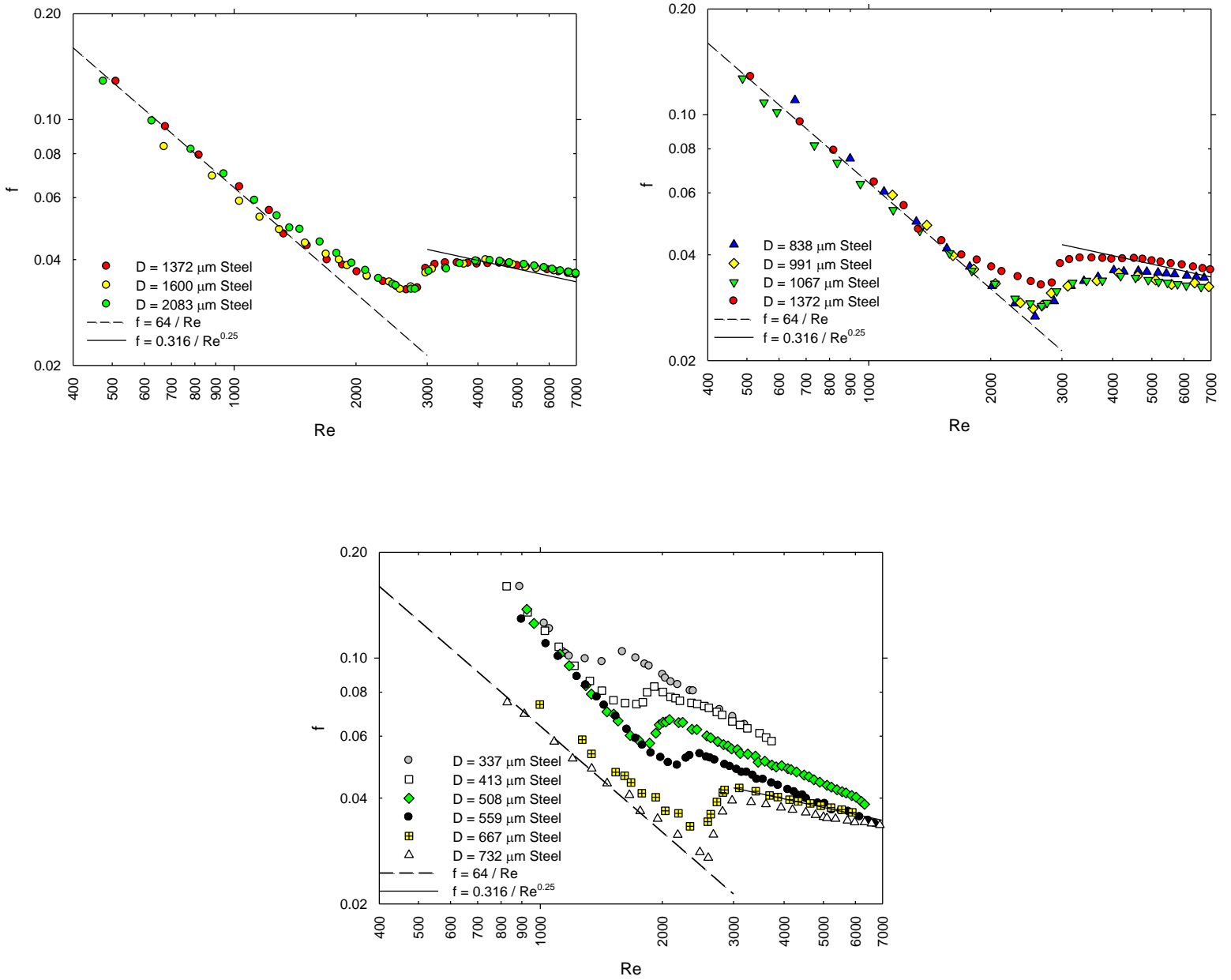


Figure 17: Effect of diameter on friction factor profile of steel tubes [Ghajar et al. (2010a)]

The result as shown in Figure 16 starts with the lowest profile in the transition region for the 762 μm tube diameter followed by the transition profiles of the 381 μm , 1016 μm and 508 μm tube diameters respectively.

In the turbulent region all the tubes followed the theoretical turbulent line. All the tubes entered the turbulent region at $\text{Re} > 3000$ along the conventional theoretical line.

Now let us consider the previous work done with low relative roughness. It should be noted that no such thorough investigation at this relative roughness range has been done. Past work provides enough evidence to support the current behavior of tubes. Table 2 lists few of the many research work accomplished in the past with low relative roughness tubes. All the listed papers are reviewed in the literature review chapter, handful of author's results and conclusions are discussed in detail here. Researchers observed that the result of all the tubes with such low relative roughness was along the theoretical lines, similar results are reported for this work. But questions like behavior of friction factor profile in the transition, transition range variation with decrease in the tube diameter were not investigated.

Experiments by Xu et al. (2000) on channels with hydraulic diameter ranging from 30 μm to 344 μm are shown in Figure 18. The figure shows that aluminum and silicon channels were in good agreement with theoretical laminar line. Remarkably a deviation from theoretical line was noted for aluminum channels but absolutely no deviation was observed for silicon channels even though silicon channels were smaller. Same phenomenon was observed for 381 μm nickel tube used in this work. It was mentioned by Xu et al. (2000), that it is quite confusing to explain such phenomena in describing the characteristics of the flow in micro channels. Transition was

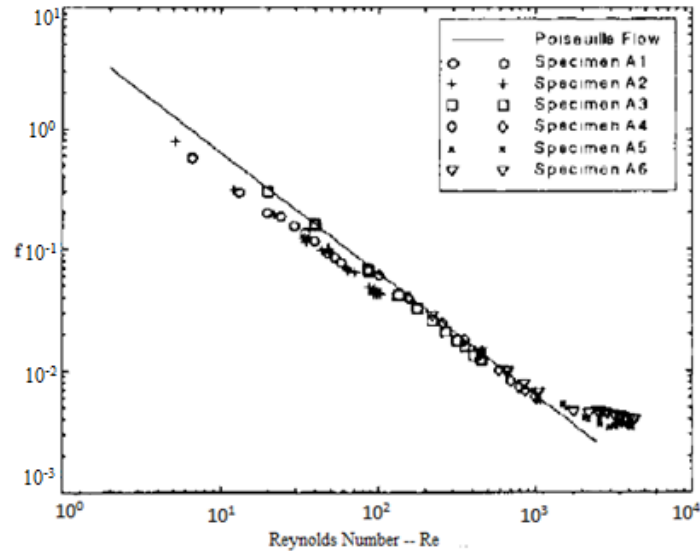
reported at around 1500 Reynolds number. Transition related doubts were not addressed by the authors.

Table 2: List of earlier work done with low relative roughness tubes/channels.

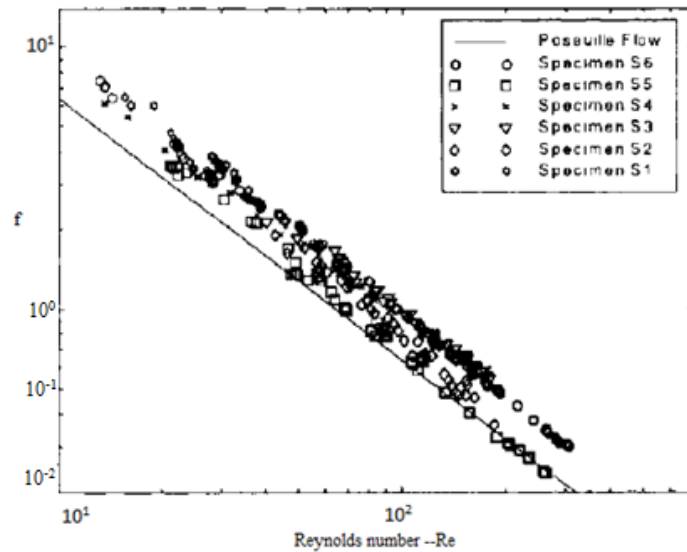
| Author/Year | Material | Diameter (μm) | Relative Roughness (%) |
|-------------------------|---------------------------|--|-------------------------------|
| Acosta et. al (1985) | S Steel (Rectangular) | 953 (smooth surface) | 0.13; 0.31; 0.21 |
| Du et. al (2000) | Glass | 79.9-166.3 | < 0.1 |
| Li et. al (2003) | Glass, Silicon | 79.9-166.3, 100.3-205.3 | <0.1 |
| Pfund et. al (2000) | Steel Channels | 128-521 | 0.57 |
| Xu et. al (2000) | Al, Silicon (Rectangular) | 46.8-344.3, 29.59-79.08 | 0.15–1 Al, Silicon 0.025–0.07 |
| Hegab et. al (2002) | Al (Rectangular) | 112-210 | 0.16–0.89 |
| Wu & Cheng (2003) | Silicon (Trapezoidal) | 25.9-291 | <0.12 |
| Phares & Smedley (2004) | Polyimide | 119&152 | <1 |
| Lorenzini et al. (2010) | Silicon, Steel | 29.9-508 | NA |
| Ghajar et al. (2010b) | Glass | 1000 | 0-0.43 |

In a similar fashion Li et al. (2003) considered glass and silicon as smooth tubes and concluded that friction factor profile remain approximately the same with the conventional theories. Figure 19 shows the friction factor versus Reynolds number plot for the tubes with diameters 80 μm to

205.3 μm . It was also mentioned that tubes' friction factor profile moves to transition along the lines of macro tubes. At this point it is important to mention that a shift in the friction factor profile was noticeable for steel tubes tested by the authors, similar to that observed by Ghajar et al. (2010a).



(a)



(b)

Figure 18: Friction factor results for (a) Aluminum, (b) Silicon channels from Xu et al. (2000)

Nevertheless the meticulous profile review of the transition region like in current work and by Ghajar et al. (2010a) was missing.

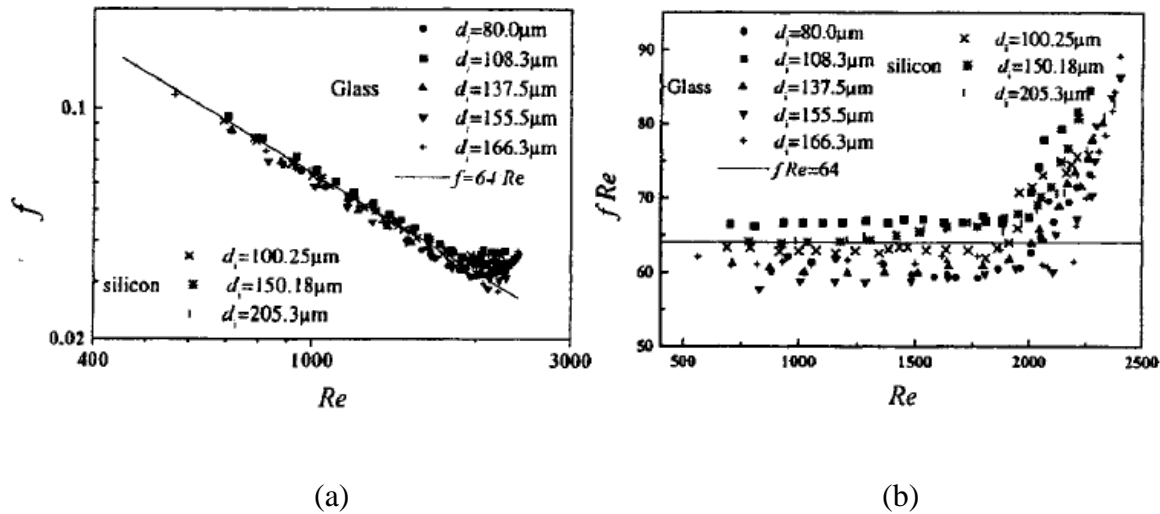
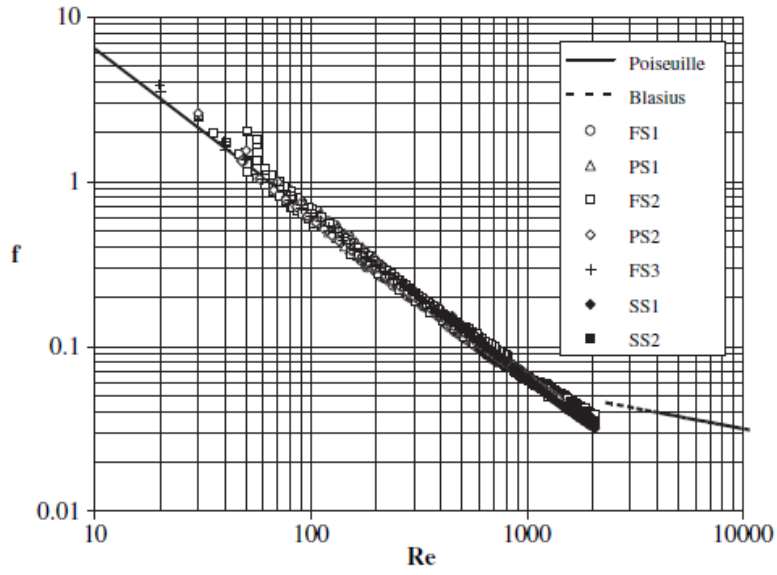
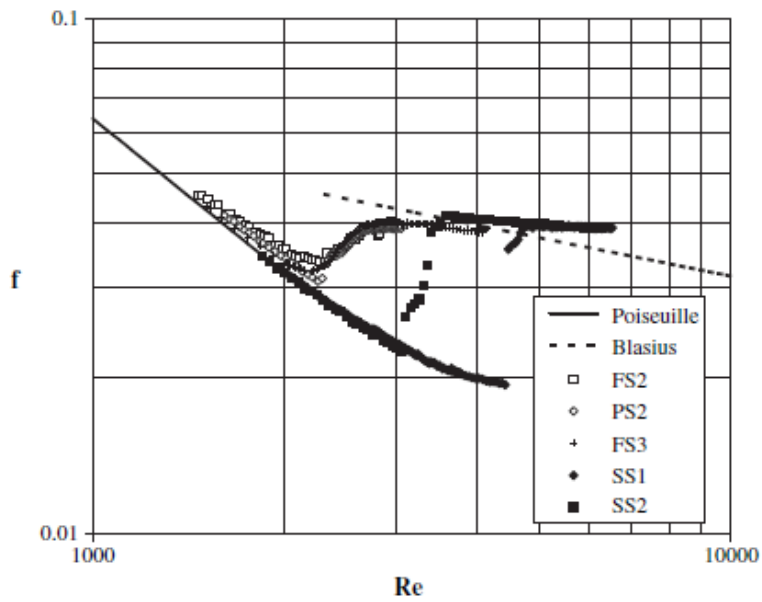


Figure 19: Glass and silicon tubes results from Li et al. (2003) (a) Friction factor results (b) fRe characteristics for the glass and silicon tubes.

Latest results by Lorenzini et al. (2010) found similar results with all tubes tested followed the theoretical lines and no shift was observed. Interestingly Lorenzini et al. (2010) found a delay in the transition for steel tube (high relative roughness) compared with fused silica (low relative roughness) tubes. Figure 20 (a) shows that there was no delay in the transition, while Figure 20 (b) illustrates the delay in the transition for steel tubes. In the present work transition of smallest diameter tube 381 μm (high relative roughness) was delayed. Wagner and Kandlikar (2012) also found inconsistencies with their experimental results it is discussed in detail in Chapter II.



(a)



(b)

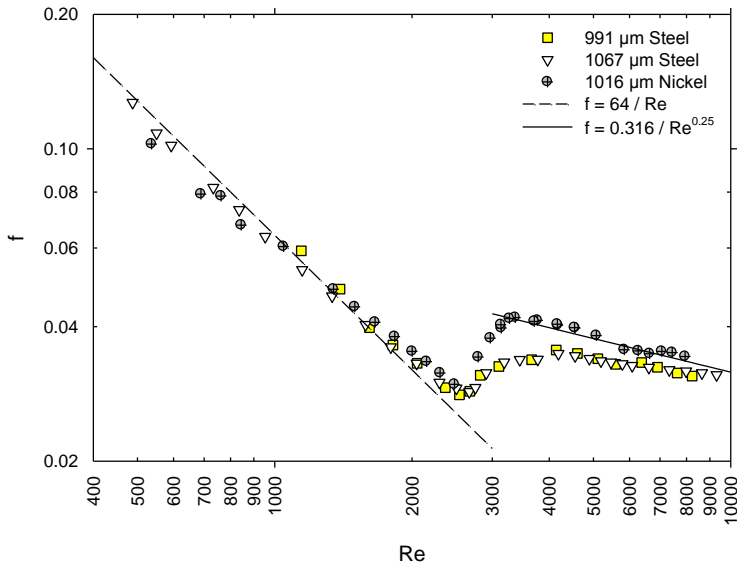
Figure 20: Friction factor and transition results for fused silica and stainless steel microtubes from Lorenzini et al. (2010) (a) Friction factor profile for fused silica and stainless steel tubes, (b) Transition for fused silica and stainless steel tubes tested

4.3 Comparison with Steel and Glass Data

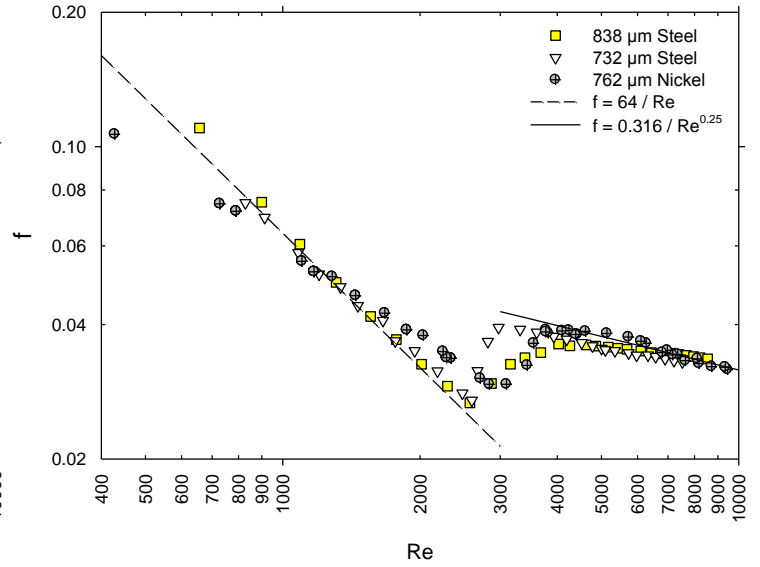
Nickel tubes experimental results were compared with steel tube experimental data of Ghajar et al. (2010a). Individual nickel tube was compared with a comparable diameter of steel tube. Figure 21 shows all the comparisons for nickel and steel tubes. The 1016 μm diameter nickel tube was assessed with 1067 μm and 991 μm diameter steel tube. The 762 μm diameter nickel tube was compared with 838 μm and 732 μm diameter steel tube. The 508 μm diameter nickel tube was compared straight away with the similar diameter available 508 μm diameter steel tube. The 381 μm diameter nickel tube was assessed with 413 μm and 337 μm diameter steel tubes.

It is clearly visible that no roughness effect was detected for the 1016 μm , 762 μm diameter nickel tubes, when compared with the corresponding steel tube diameters. The 1016 μm diameter nickel tube followed the corresponding steel tubes in the laminar region very well, both of the tubes sticking with the laminar theoretical line. For the 762 μm diameter nickel it was observed that although no prominent roughness effect was observed, but the 762 μm diameter nickel deviated from the laminar line earlier than steel tube.

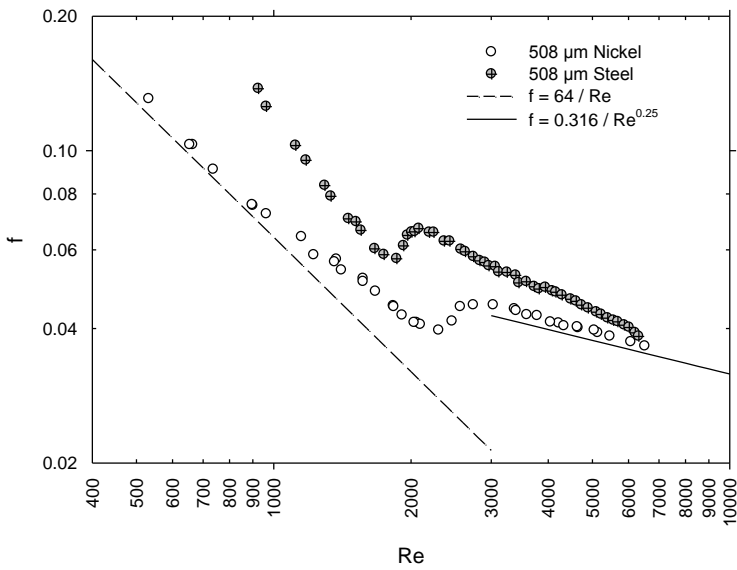
But roughness effect is evident from the 508 μm nickel tube. The 508 μm and 381 μm nickel tubes sit on the laminar line but the steel counter parts are greater than 40% higher than the theoretical laminar line. This supports with the Ghajar et al. (2010a) observations that roughness effect in friction factor profile was visible below 667 μm and after.



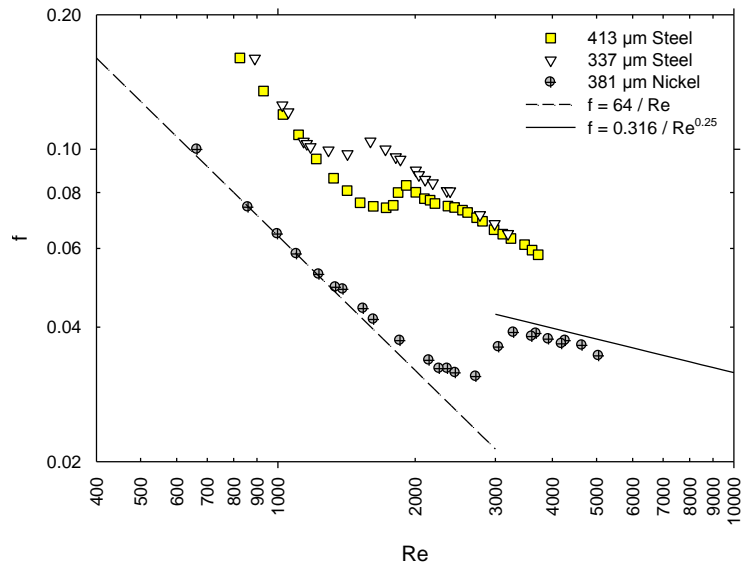
(a)



(b)



(c)



(d)

Figure 21: Comparison of experimental results for nickel tubes with steel tubes (a) 1016 μm nickel tube, (b) 762 μm nickel tube, (c) 508 μm nickel tube and (d) 381 μm nickel tube

Glass tubes experimental data obtained from Ghajar et al. (2010b) was also examined against the nickel tube experimental values. The 1016 μm diameter of nickel tube was compared with the 1000 μm glass data. Pressure drop reading were collected only for 1000 μm glass tubes with relative roughness ranging from 0 to 0.0043. Figure 22 shows comparison of selected 1016 μm nickel tube with all the glass tubes data available. But no roughness effect was noticed as the nickel as well the glass tubes followed the theoretical lines.

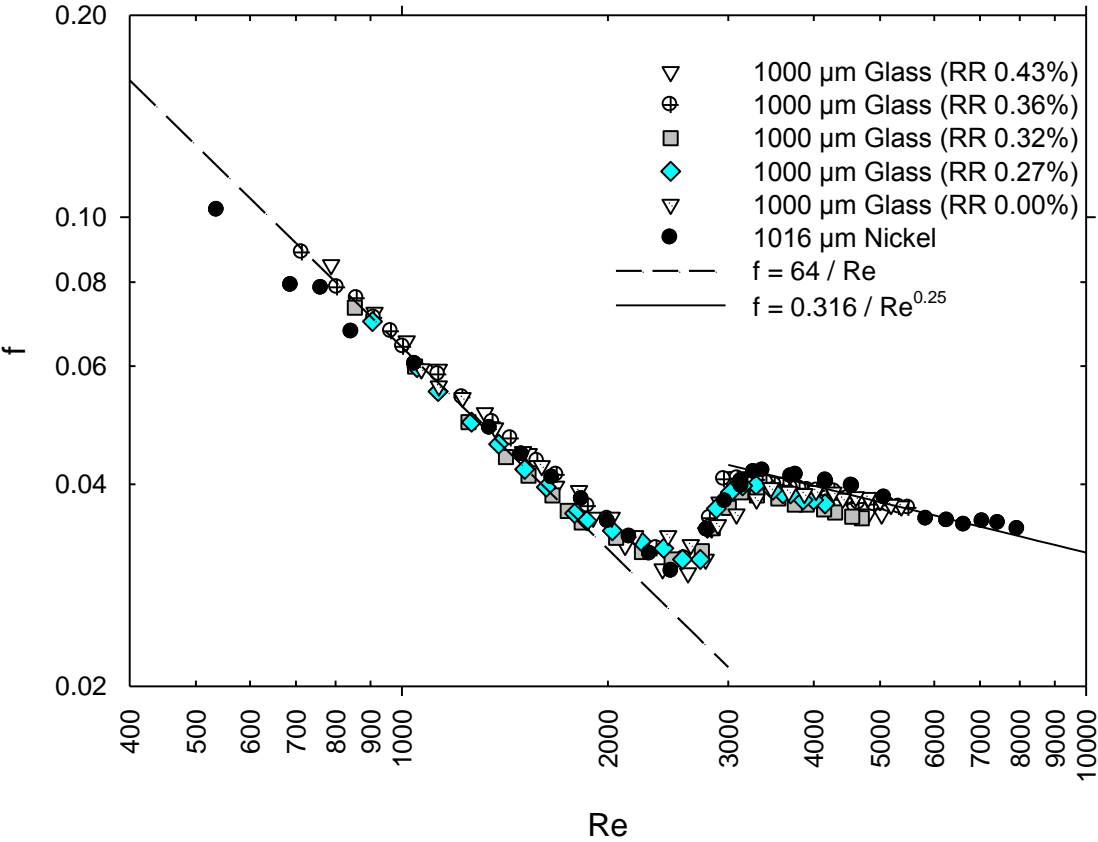


Figure 22: Comparison of 1016 μm diameter nickel tube with 1000 μm glass tube

4.4 Roughness Effect in Laminar Region

As discussed in the previous chapters about the constricted parameters proposed by Kandlikar et al. (2005) and the claimed better prediction of flow in the laminar region was put to test. Only the tubes which were roughest and showed the deviation from the laminar line were examined. Based on this criterion there are four tubes which were appropriate choice the 559 μm , 508 μm , 413 μm and 337 μm diameter steel tubes from Ghajar et al. (2010a). Figure 23 shows difference between experimental data when plotted without using constricted parameters, and when plotted using the constricted flow friction factor (f_{cf}) and Reynolds number (Re_{cf}).

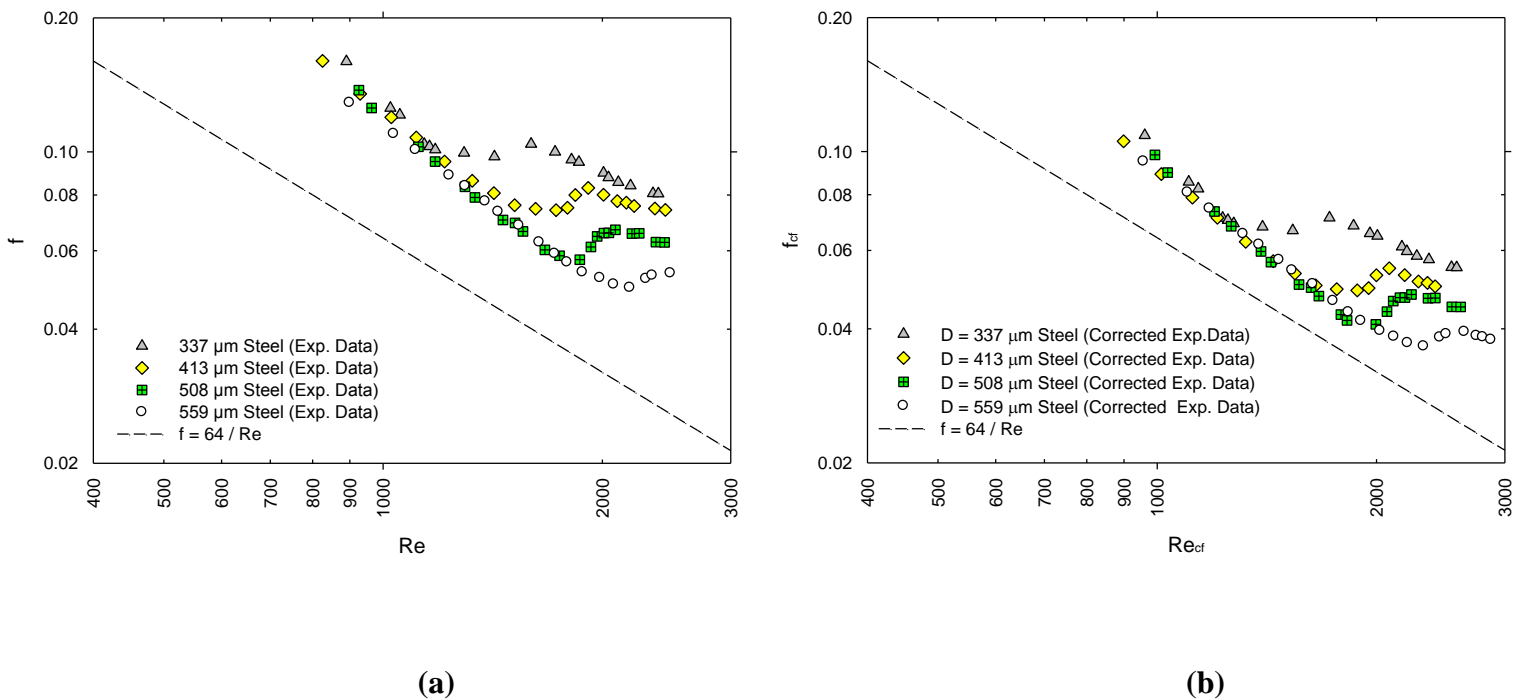


Figure 23: Experimental data for selected steel tubes for comparison with the theoretical laminar region friction factor (a) Original steel data (b) Steel data plotted with constricted parameters

In above figure for part (b) data points were obtained using Equations (10) and (11) on Reynolds number and friction factor data of steel tubes. Equations are discussed in detail in the previous chapter. It was expected that upward shift observed in the friction factor profile of the four roughest steel tubes will be compensated by constricted flow parameters. This improvement was observed by Kandlikar et al. (2005) for micro channel with hydraulic diameter 953 μm and relative roughness 7.3%. Similar observations were reported by Brackbill and Kandlikar (2007) for relative roughness ranging from 1.42% to 4.88% and hydraulic diameter ranging from 198 μm to 1084 μm . It should be noted that above mentioned observations were from micro channels only. Authors did not employ constricted parameters idea on micro tubes. When the data for these four steel tubes was compared with laminar theoretical line ($f=64/\text{Re}$), it was found that friction factor was reduced considerably for the four roughest tubes (refer to Table 3) by use of constricted flow parameters. But the observed laminar region for the tubes in question was not following the theoretical laminar line as observed by Brackbill and Kandlikar (2007). This puts a question mark on the effectiveness of constricted parameters prediction of friction factor in laminar region for the micro tubes.

Table 3: Lists error in friction factor values from the theoretical laminar line with and without correction factors

| Tube Diameter (μm) | Relative Roughness ϵ/D (%) | Approximate Error from theoretical Laminar line | |
|---------------------------------|-------------------------------------|---|---------------------------------------|
| | | % Error with correction | % Error without correction (Original) |
| 559 | 2.95 | 20% | 40% |
| 508 | 3.25 | 15% | 40% |
| 413 | 4 | 22% | 44% |
| 337 | 3.77 | 26% | 47% |

4.5 Correlations for Estimation of Critical Reynolds Number in Microtubes

Chapter III explains how Brackbill & Kandlikar (2007) developed a correlation for prediction of critical transition Reynolds number in micro channels. Similar attempts were made for friction factor data available for nickel tubes, steel tubes by Ghajar et al. (2010a) and glass tubes by Ghajar et al. (2010b). The available data provides critical Reynolds number from relative roughness 0% to 4%. Before moving on to the elaboration of the correlation development it is important to check the correlation proposed by Brackbill & Kandlikar (2007) on the present data set available. Figure 24 shows the critical Reynolds number for the nickel, steel and glass tubes compared with Equation (12).

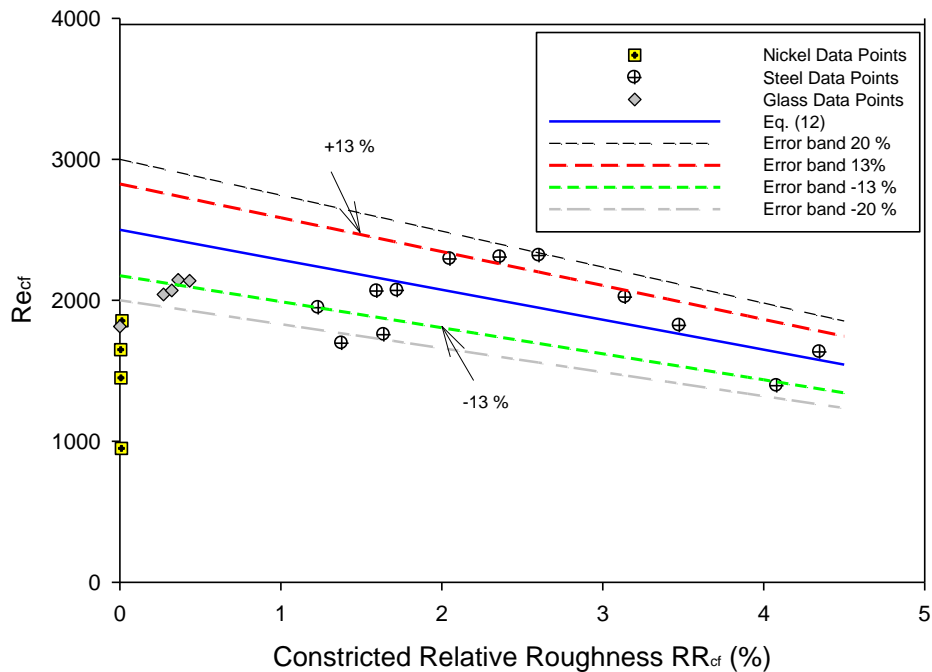


Figure 24: Critical Reynolds numbers for the data set available compared with Equation (12) proposed by Brackbill and Kandlikar (2007)

Comparison shows that correlation did not show the favorable behavior with current data sets, particularly in the low relative roughness area. It was observed that good number of the steel points were in the $\pm 13\%$ error range of the Equation (12) as reported by Brackbill and Kandlikar (2007). Similar was the case for two data points of glass with higher relative roughness, but it was not observed for lower relative roughness data points of glass and nickel. Lower relative roughness measured data points were below the -13% error range. More importantly increasing relative roughness in the range did not drop critical Reynolds number as distinguished by authors. Rather an increase in critical Reynolds number was observed for most of the points up till 2.6% relative roughness. It is contrary with the trend observed between critical Reynolds number and relative roughness by Brackbill and Kandlikar (2007). Equation (12) was based upon this opposite trend observed by the authors.

Brackbill and Kandlikar (2007) look at the critical Reynolds number data over a very broad range (0 - 30%) of relative roughness. Based on this wide range authors propose that critical Reynolds number decreases with increase in relative roughness. Whereas a closer look at short range from 0 to 4% indicates a different trend for critical Reynolds number with respect to relative roughness.

For constricted relative roughness ($0\% \leq RR_{cf} < 2\%$) which is considerably a good range for all the data points that were below the Equation (12) line. A better curve fit is characterized by ample data points on both sides of curve fit. Moreover average absolute error was found to be 27.13% which is quite higher than 13% reported by Brackbill and Kandlikar (2007). Also it cannot be overlooked that the Equation (12) proposed by Brackbill and Kandlikar (2007) is based on limited data, and the data are only from micro channels. Above assessment suggests

that for the micro tubes correlation recommended for prediction of critical Reynolds number, based on the data collected in micro channels is crude in nature and not sufficient.

Table 4 lists for the glass and steel data points the critical Reynolds number and corresponding critical constricted Reynolds number predicted by Equation (12). It is evident from the table that for glass tube with increasing relative roughness critical Reynolds number (Re_{cf}) increases. Similar was the case for steel tubes up till 2.6% relative roughness.

Table 4: Lists critical Reynolds number measured experimentally and critical constricted Reynolds number calculated for glass and steel tubes.

| Material | Diameter (μm) | RR_{cf} (%) | Re_{cf} (Experimental) | $Re_{c,cf}$ (Calculated) |
|-----------------|--|-------------------------------------|--|--|
| Glass | 1000 | 0.0000 | 1815.00 | 2500.00 |
| Glass | 1000 | 0.2715 | 2041.45 | 2442.31 |
| Glass | 1000 | 0.3221 | 2070.18 | 2431.56 |
| Glass | 1000 | 0.3626 | 2144.44 | 2422.95 |
| Glass | 1000 | 0.4337 | 2138.65 | 2407.83 |
| Steel | 2083 | 1.3783 | 1695.42 | 2207.11 |
| Steel | 1600 | 1.6396 | 1756.19 | 2151.59 |
| Steel | 1372 | 1.2330 | 1947.71 | 2237.98 |
| Steel | 1067 | 1.5967 | 2065.44 | 2160.69 |
| Steel | 991 | 1.7234 | 2070.22 | 2133.77 |
| Steel | 838 | 2.0510 | 2293.58 | 2064.17 |
| Steel | 732 | 2.3620 | 2307.16 | 1998.07 |
| Steel | 667 | 2.6042 | 2317.30 | 1946.61 |
| Steel | 559 | 3.1401 | 2022.32 | 1832.73 |
| Steel | 508 | 3.4759 | 1821.94 | 1761.36 |
| Steel | 413 | 4.3478 | 1633.58 | 1576.09 |
| Steel | 337 | 4.0810 | 1394.68 | 1632.79 |

Nickel was not taken into account while proposing the correlations. Since the nickel tubes have very low relative roughness, the data points lie almost on y-axis of the plot. This does not add

any significant benefit in correlation development.

Three different ranges were recommended for prediction of critical Reynolds number in micro tubes on the basis of present data sets available. First range from relative roughness 0 to 0.5%, second range for 1% - 2% relative roughness, and third range from 2 to 4% relative roughness of available micro tube data. Figure 25 shows the first range with the glass tubes critical Reynolds numbers points.

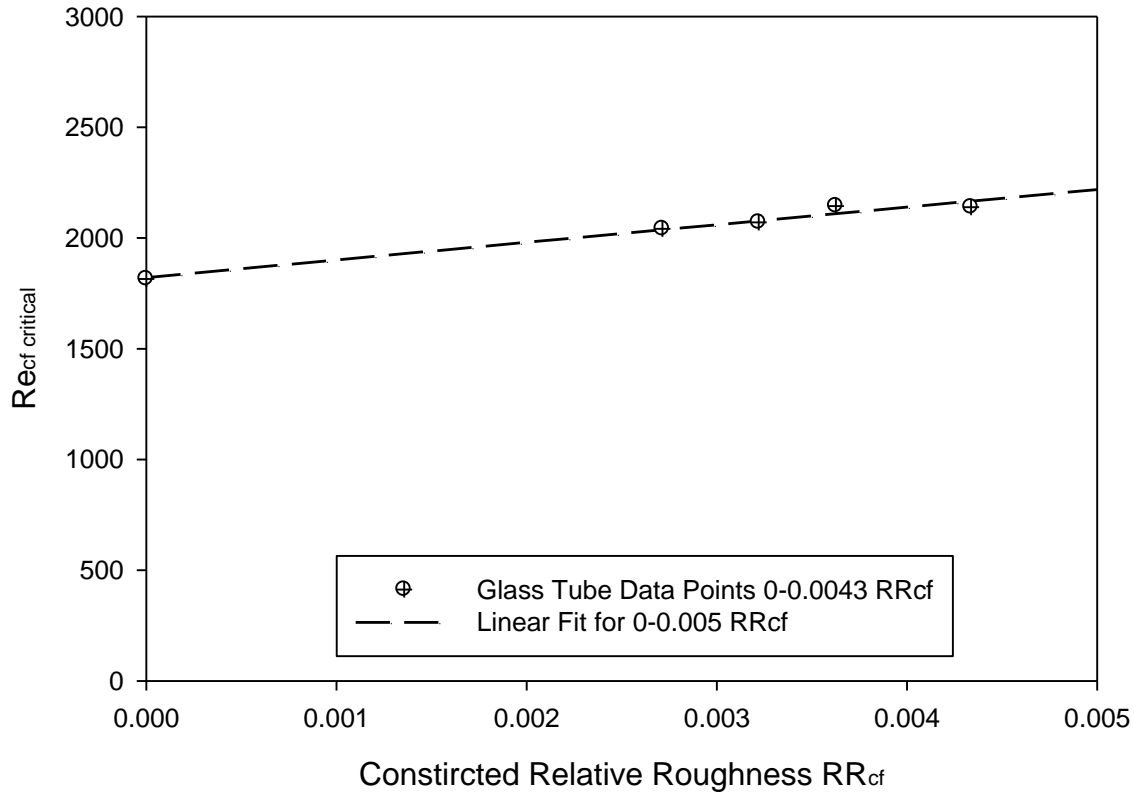


Figure 25: Linear fit for 0 to 0.005 RR_{cf} (0-0.5% RR_{cf}) or (0 to 0.5% relative roughness) data points

Equation for 0 to 0.005 RR_{cf} (0-0.5% RR_{cf}) range is;

$$0 \leq \frac{\varepsilon}{D_{h,cf}} < 0.005 \quad Re_{c,cf} = \frac{405}{0.005} (\varepsilon/D_{h,cf}) + Re_o \quad (14)$$

Where Re_o is transition for $\varepsilon/D_{h,cf} = 0$;

$Re_o = 1815$ for this work. Average absolute error for above correlation was found to be 0.9%.

Figure 26 shows the other two ranges with the steel tubes critical Reynolds number points.

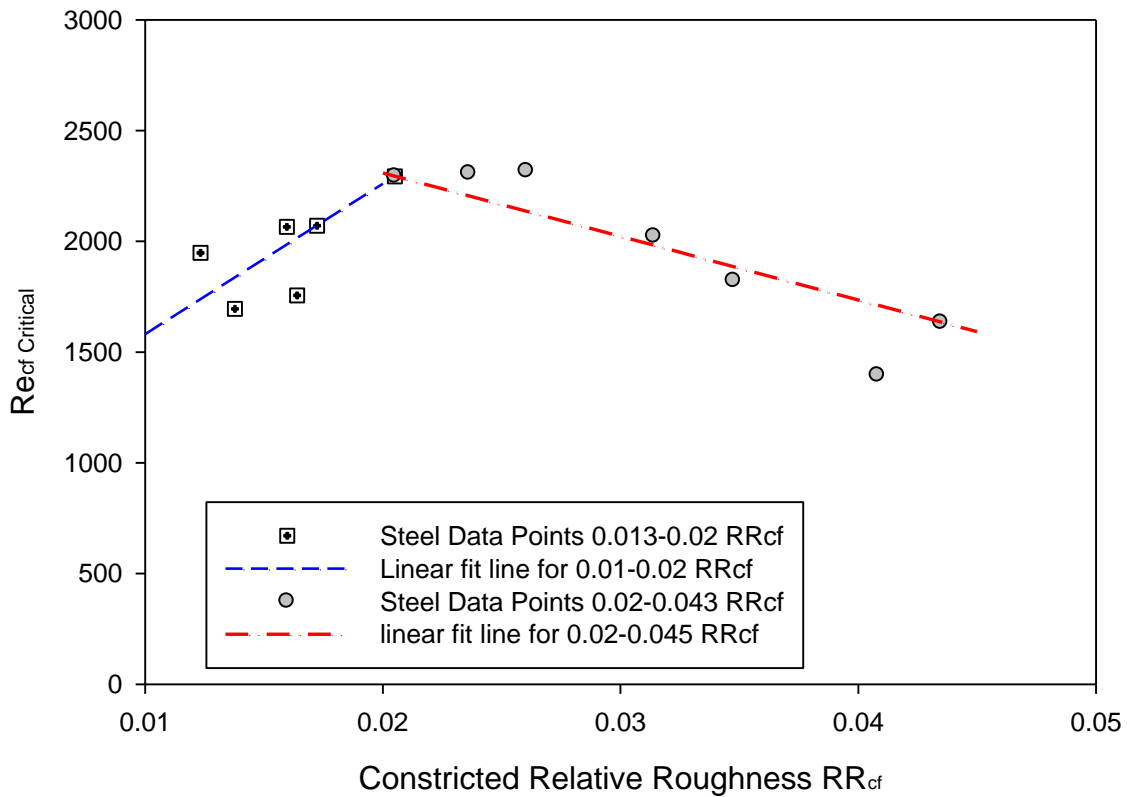


Figure 26: Linear fit for 0.01 to 0.045 RR_{cf} (0.01-0.045% RR_{cf}) or (1 to 4% relative roughness) data points

Equations for the two ranges are given below;

$$0.01 < \frac{\varepsilon}{D_{h,cf}} \leq 0.02 \quad Re_{c,cf} = \frac{679}{0.01} (\varepsilon/D_{h,cf} - 0.01) + 1581 \quad (15)$$

Average absolute error for Equation (15) was found to be 6.3%.

$$0.02 \leq \frac{\varepsilon}{D_{h,cf}} < 0.045 \quad Re_{c,cf} = \frac{-574}{0.02} (\varepsilon/D_{h,cf} - 0.02) + 2306 \quad (16)$$

Average absolute error for Equation (16) was obtained as 5.8%.

Cumulative average absolute percentage error of 6% was calculated for the data points with respect to the new equations, which is a significant improvement from 27.13% by using equation (12). This error is much lower than the 13% error reported by Brackbill and Kandlikar (2007).

CHAPTER V

CONCLUSION & RECOMMENDATIONS

In this research work pressure drop experiments were performed on very low relative roughness (0.005 - 0.013%) nickel tubes. Diameters were 1016 μm , 762 μm , 508 μm and 381 μm and their friction factor profiles were studied. Next part of the work was to analyze the effect of constricted flow parameters proposed by Kandlikar et al. (2005), in laminar region on the available data sets. Subsequently based on the constricted parameters and data set available, a set of correlations were proposed for prediction of critical Reynolds number in micro tubes.

Selection of correct diaphragm for pressure drop measurement plays an important role in this type of research. Study was done on nickel tubes with diaphragms of capacities 1379 kPa – 55.1 kPa. Resembling trend in shift of friction factor profile was observed for nickel tubes when compared with the observation of Ghajar et al. (2010a) for steel tubes. Nevertheless friction factor profile shift was not as substantial as noted by authors for steel tubes. Thus, selection of diaphragm significantly affects rough tubes, but effect starts declining with decrease on relative roughness although never completely diminishes.

In steel tubes from Ghajar et al. (2010a) there was a delay in transition with decrease in diameter but this was not the case for nickel tubes. Critical Reynolds number reduced with decrement in diameter for 1016 μm , 762 μm & 508 μm . For 381 μm nickel tube a reverse trend was observed.

Lorenzini et al. (2010) concluded that with decrease in diameter transition is delayed for rough tubes. Similar trend was observed for 381 μm which is the roughest tube of the group. But this data is insufficient to make any judgment for transition delay in such low relative roughness tubes. To make a firm conclusion more tubes with low diameters and low relative roughness need to be studied.

Experimental results for friction factor of nickel were found to be in good agreement with theoretical lines. Role of roughness was not witnessed in nickel tubes. Parallel upward shift for friction factor profile was not seen, which was expected as tubes were very smooth. An irregular pattern in friction factor profile with change in diameter in transition region was observed. Researches till now haven't studied friction factor profile pattern with change in diameter for smooth tubes. To reach a strong conclusion like Ghajar et al. (2010a) in transition more work is required with numerous diameters of smooth tubes.

Results of nickel tubes were compared with available steel and glass data. Roughness effect for steel tubes was only visible below 667 μm and after. Whereas with glass tubes no roughness effect was observed at all. This backs the observation by Ghajar et al. (2010a) that friction factor profile depends upon roughness and the tube diameter. High roughness and low tube diameter triggers the roughness effect on friction factor profile for fluid flow through micro tubes.

Supposition of no roughness effect in laminar region was overruled by using constricted parameters proposed by Kandlikar et al. (2005). But this concept of overlooking the roughness element height and considering a free flow area seemed to be under-developed in nature. It definitely improves the friction factor in laminar region as it can be observed in Figure 23. However for micro tubes even after correction friction factor profile did not lie on theoretical

laminar line. This directs that more work is required to establish the constricted theory for improving the roughness in laminar region.

Furthermore it was observed that correlations suggested by Brackbill and Kandlikar (2007) for prediction of critical Reynolds number was basic in nature as well. Correlations were proposed on a wide relative roughness range with data based only on micro channels. As discussed in previous chapter the correlation appears to be in elementary stage when employed for the data sets obtained experimentally. The correlation (12) was broken up in three different parts and was improved for prediction of critical Reynolds number in 0 to 4% relative roughness range.

This research has justified reasonable points from the previous works and also has opened up new areas of work. It was established that sensitivity of instrumentation plays high role in obtaining correct results. It was observed that there is no roughness effect for low relative roughness (0.005 - 0.013%) tubes as expected. But for any rational conclusion in transition region behavior more work is required. It can be established from this current work that constricted parameters is promising. But it requires to be investigated with more data sets with varied shape and size to develop it. The correlations (12) and (13) represent channels with wide range of relative roughness. To verify and generalize the correlation for fluid flow through all micro shapes more data with varied relative roughness is required.

REFERENCES

- Acosta, R. E., Muller, R. H., Tobias, C. W. "Transport Process in Narrow (Capillary) Channels." *AICHE Journal* 31, no. 3 (March 1985): 473-482.
- Araki, T., Kim, M.S., Iwai, H., Suzuki, K. "Minichannels in Polymer Electrolyte Membrane Fuel Cells." *Microchannels and Minichannels*, 2002: 117-130.
- Arkilic, E., Schmidt, M., Breuer, K. "Gaseous Slip Flow in Microchannels." *Application of Microfabrication*. Chicago, IL: ASME, 1994. 57-65.
- Baviere, R., Ayela, F., Person, S. Le., Favre-Marinet, M. "An Experimental Study of Water Flow in Smooth and Rough Rectangular Micro-Channels." *Microchannels and Minichannels*. Rochester, New York, 2004.
- Brackbill, T. P., Kandlikar, S. G. "Effect of Triangular Roughness Elements on Pressure Drop and Laminar-Turbulent Transition in Microchannels and Minichannels ." *Proceedings of International Conference on Nanochannels, Microchannels and Minichannels* . 2006.
- Brackbill, T. P., kandlikar, S. G. "Effects of Low Uniform Relative Roughness on Single Phase Friction Factors in Microchannels and Minichannels." *International Conference on Nanochannels, Microchannels and Minichannels* . Puebla, Mexico, 2007.
- Brutin, D., Tardist, L. "Experimental Friction Factor of a Liquid Flow in Microtubes." *Physics of Fluids*, 2003: 653-661.
- Celeta, G. P., Cumo, M., Guglielmi, M., Zummo, G. "Experimental Investigation of Hydraulic and Single Phase Heat Transfer in 0.130-MM Capillary Tube." *Microscale Thermophysical Engineering*, 2002: 85-97.
- Choi, S. B., Barron, R. F., Warrington, R. O. "Fluid flow and heat transfer in microtubes." *ASME Micromechanical Sensors, Actuators and Systems DSC-32* (1991): 123-134.
- Errol, A. B., Breuer, K. S., Schmidt, M. A.,. "Gaseous Flow in Microchannels." *Application of Microfabrication to Fluid Mechanics*, 1994: 57-66.

- Ghajar, A. J., Tang, C. C., Cook, W. L. "Experimental Investigation of Friction Factor in The Transition Region for Water Flow in Mini tubes and Micro tubes." *Heat Transfer Engineering*, 2010a: 644-657.
- Ghajar, A. J., Wen , Q., Tam, L. M., Tam , H. K. "The Effect of Inner Surface Roughness on Friction Factor in Horizontal Microtubes." *International Conference on Mechanical and Electronics Engineering*. Kyoto, Japan, 2010b.
- Han, D., Lee, Kyu-Jung. "Investigation of Single Phase Frictional Pressure Loss in Circular Micro tubes." *Mechanical Science and Technology*, 2006: 1284-1291.
- Harley, J. C., Huang, Y., Bau, H. H., Zemel, J. N. "Gas Flow in Micro-Channels." *Journal of Fluid Mechanics*, 1995: 257-274.
- Hegab, H. E., Bari, A., Ameen, T. "Friction and convection studies of R-134a in microchannels within the transition and turbulent flow regimes." *Experimental Heat Transfer* 15 (2002): 245-259.
- Kandlikar, S. G. "Roughness effects at microscale-reassessing Nikuradse's experiments on liquid flow in rough tubes." *Bulletin of the Polish Academy of Sciences - Technical Sciences* 53, no. 4 (2005): 343-349.
- Kandlikar, S. G., Schmitt, D., Carrano, A. L., Taylor, J. B. "Characterization of Surface Roughness Effects on Pressure Drop in Single Phase Flow in Minichannels." *Physics of Fluids*, 2005.
- Kline, S. J., McClintock, F. A. "Describing uncertainties in single-sample experiments." *Mechanical Engineering* 75, no. 1 (1953): 3-8.
- Krishnamoorthy, C., Ghajar, A. J. "Single-Phase friction factor in micro-tubes: a critical review of measurement, instrumentation and data reduction techniques from1991-2006." *Proceedings from 5th International Conference on Nanochannels, Microchannels and Minichannels*. Puebla, Mexico, 2007.
- Li, Z. X., Du, D. X., Guo, Z. Y.,. "Experimental Study on FLOW Characteristics of Liquid in Circular Microtubes." In *Nanoscale and Microscale Thermophysical Engineering*, 253-265. Beijing, 2003.
- Lorenzini, M., Morini, G., Salvini, S. "Laminar, transitional and turbulent friction factors for gas flows in smooth and rough microtubes." *International Journal of Thermal Sciences*, 2010: 248-255.
- Mala, G. M., Li, D. "Flow characteristics of water in micro tubes." *International Journal of Heat and Fluid Flow*, 1999: 142-148.
- Nikuradse, J. "Law of Flow in Rough Pipes." *National advisory committee for aeronautics - Technical Memorandum 1292*, 1933.

- Papautsky, I., Brazzle, J., Ameal, T., Frazier, B. A. "Laminar fluid behavior in microchannels using micropolar fluid theory." *Sensors and Actuators*, 1999: 101-108.
- Peng, X. F., Peterson, G. P., Wang, B. X. "Frictional Flow Characteristics of Water Flowing Through Rectangular Microchannels." *Experimental Heat Transfer*, 1994: 249-264.
- Pfahler, J., Harley, J., Bau, H. H., Zemel, J. N. "Liquid and gas transport in small channel." *Microstruct. Sensor actuator*, 1991: 149-157.
- Pfund, D., Rector, D., Shekarriz, A., Popescu, A., Welty, J. "Pressure Drop Measurements in a Microchannel." *AIChE Journal* 46, no. 8 (August 2000): 1496-1507.
- Phares, D. J., Smedley, G. T. "A study of laminar flow of polar liquids through circular microtubes." *PHYSICS OF FLUIDS* 16, no. 5 (May 2004): 1267-1272.
- Tang, G. H., He, Y. L., Tao, W. Q., Li, Z. "Experimental and numerical studies of liquid flow and heat transfer in microtubes." *International Journal of Heat and Mass Transfer*, 2007a: 3447-3460.
- Tang, G. H., Li, Z., He, Y. L., Tao, W. Q. "Experimental study of compressibility, roughness and rarefaction influences on microchannel flow." *International Journal of Heat and Mass Transfer*, 2007b: 2282-2295.
- Wagner, R. N., Kandlikar, S. G. "Effects of Structured Roughness on Fluid Flow at the Microscale Level." *Heat Transfer Engineering* 33, no. 6 (2012).
- Wu, A. P., Little, W. "Measurement of friction factor for the flow of gases in very fine channels used for micro miniature Joule-Thompson refrigerators." *Cryogenics* 23, no. 6 (1983): 273-277.
- Wu, H. Y., Cheng, P. "Friction factors in smooth trapezoidal silicon microchannels with different aspect ratio." *International Journal of Heat and Mass Transfer* 46 (2003): 2519-2525.
- Xu, B., Ooi, K. T., Wong, N. T., Choi, W. K. "Experimental Investigation of Flow Friction for Liquid Flow in Microchannels." *Int. Comm. Heat Mass Transfer*, 2000: 1165-1176.
- Yu, D., Ameal, T., Warrington, R., Barron, R.,. "An Experimental and Theoretical Investigation of Fluid Flow and Heat Transfer in Microtubes." *ASME-JSME Thermal Engineering Joint Conference*. Tokyo: Japan Society of Mechanical Engineering, 1995. 523-530.
- Zhigang, L., Yaohua, Z. "Experimental study on visualization of the flow field in microtube." *Engineering and Materials Sciences*, 2005: 521-529.
- Tang, G. H., He, Y. L., Tao, W. Q., Li, Z. "Experimental and numerical studies of liquid flow and heat transfer in microtubes." *International Journal of Heat and Mass Transfer*, 2007a: 3447-3460.

- Tang, G. H., Li, Z., He, Y. L., Tao, W.Q. "Experimental study of compressibility, roughness and rarefraction influences on microchannel flow." *International Journal of Heat and Mass Transfer*, 2007b: 2282-2295.
- Wagner, R. N., Kandlikar , S. G. "Effects of Structured Roughness on Fluid Flow at the Microscale Level." *Heat Transfer Engineering* 33, no. 6 (2012).
- Wu, A. P., Little, W. "Measurement of friction factor for the flow of gases in very fine channels used for micro miniature Joule-Thompson refrigerators." *Cryogenics* 23, no. 6 (1983): 273-277.
- Wu, H. Y., Cheng, P. "Friction factors in smooth trapezoidal silicon microchannels with different aspect ratio." *International Journal of Heat and Mass Transfer* 46 (2003): 2519-2525.
- Xu, B., Ooi, K. T., Wong, N. T., Choi, W. K. "Experimental Investigation of Flow Friction for Liquid Flow in Microchannels." *Int. Comm. Heat Mass Transfer*, 2000: 1165-1176.
- Yu, D., Ameel, T., Warrington , R., Barron, R.,. "An Experimental and Theoretical Investigation of Fluid Flow and Heat Transfer in Microtubes." *ASME-JSME Thermal Engineering Joint Conference*. Tokyo: Japan Society of Mechanical Engineering, 1995. 523-530.
- Zhigang, L., Yaohua, Z. "Experimental study on visualization of the flow field in microtube." *Engineering and Materials Sciences*, 2005: 521-529.

VITA

Atul Singh

Candidate for the Degree of

Master of Science

Thesis: EXPERIMENTAL INVESTIGATION OF FRICTION FACTOR IN MICROTUBES AND DEVELOPMENT OF CORRELATIONS FOR PREDICTION OF CRITICAL REYNOLDS NUMBER

Major Field: MECHANICAL ENGINEERING

Biographical:

Personal Data: Born in Allahabad (India) on Feb 12th, 1986. Son of Ajay Kumar Singh and Abha Singh.

Education:

2008 – 2011 Oklahoma State University, Stillwater, OK.
Master of Science in Mechanical Engineering.

2004 – 2008 Rajiv Gandhi Technical University, India
Bachelor of Engineering in Mechanical Engineering.

Experience:

2008 – 2009 Graduate Teaching Assistant, Oklahoma State University.

Professional Memberships:

American Society of Heating Refrigerating and Air-Conditioning Engineers (ASHRAE), Oklahoma State University Student Branch.

Name: Atul Singh

Date of Degree: December, 2011

Institution: Oklahoma State University

Location: Stillwater, Oklahoma

Title of Study: EXPERIMENTAL INVESTIGATION OF FRICTION FACTOR IN
MICROTUBES AND DEVELOPMENT OF CORRELATIONS FOR
PREDICTION OF CRITICAL REYNOLDS NUMBER

Pages in Study: 78

Candidate for the Degree of Master of Science

Major Field: Mechanical Engineering

Scope and Method of Study: Pressure driven flows through the micro tubes have flow characteristics of their own, which is not supported by any established macro flow theories. It was observed that, surface roughness plays major role in this variation from established theories. In this research, prime objective is to study the friction factor behavior for low relative roughness (0.005-0.013%) nickel tubes. Friction factor behavior was studied for laminar, transition and turbulent regions. Particularly the study concentrated in the start and end of the transition region and change of transition friction factor with diameter for low relative roughness tubes. Additionally the laminar region friction factor which has been conceded as no roughness area was investigated using constricted parameters. Furthermore correlations for prediction of critical Reynolds number were proposed for micro tubes with relative roughness range of 0 to 4%.

Findings and Conclusions: From this work it was established that sensitivity of instrumentation plays significant role in obtaining correct results. It was observed that there is no roughness effect in friction factor for low relative roughness nickel tubes. But for any rational conclusion in transition region behavior for low relative roughness tubes more work is required. It can be established from current work that constricted parameters are promising for improvement of laminar region friction factor. But it requires to be investigated with more data sets with varied shape and size to develop it. Correlations proposed for prediction of critical Reynolds number in microtubes worked very well with cumulative absolute average error of 6%. To verify and generalize the correlations for fluid flow through all micro shapes more data with varied relative roughness is required.

ADVISER'S APPROVAL: Afshin J. Ghajar